REFERENCES

Breitbach, M. and Bathen, D. 2001. Influence of ultrasound on adsorption processes, Ultrason. Sonochem., 8(3), 277–283.

Breitbach, M. Bathen, D. and Schmidt-Traub, H. 2003. Effect of ultrasound on adsorption and desorption processes, Ind. Eng. Chem. Res.,42(22):5635–5646.

Cacciola, G. and Rustuccia, G. 1994. Heat recovery system and CHP, 14(4):409-420.

Critoph, R.E. 1998. Performance limitations of adsorption cycles for solar cooling, Sol. Energy, 41(1): 21-31.

Diter, B. 2003. Physical waves in adsorption technology: an overview, Sep. Purif. Technol., 33(2):163–177.

Hamdaoui, O. Naffrechoux, E. Tifouti, L. and Petrier, C. 2003. Effect of ultrasound on adsorption–desorption of p-chlorophenol on granular activated carbon, Ultrason. Sonochem., 10(2):109–114.

Juang, R.S. Lin, S.H. and Cheng, C.H. 2006. A liquid-phase adsorption and desorption of phenol onto activated carbons with ultrasound, Ultrason. Sonochem., 13(3):251–260.

Leong, K.C. and Liu, Y. 2004. Numerical modeling of combined heat and mass transfer in the adsorbent bed of a zeolite/water cooling system, Appl, Therm. Eng., 24(16):2359-2374.

Lu. Y.Z. Wang, R.Z. Jianzhou, S. Xu, Y.X. and Wu, J.Y. 2004. Practical experiments on an adsorption air conditioner powered by exhaust heat from a diesel locomotive, Apply Thermal Eng, 24: 1051-1059.

Li, M. Wang, R.Z. Xu, Y.X. Wu, J.Y. and Dieng, A.O. 2002. Experiment study on dynamic performance analysis of a flat-plate solar solid-adsorption refrigeration for ice maker, Renewable energy, 27: 211-221.

Maggio, G. Freni, A. and Restuccia, G. 2006. A dynamic model of heat and mass transfer in a double-bed adsorption machine with internal heat recovery. Int. J. Refrig., 29(4):589-600.

Mason, T.J. 1991. Practical Sonochemistry: User's guide to applications in chemistry and chemical engineering, Ellis Horwood, Chichester, UK.

Penn, R. Yeager, E. and Hovorka, F. 1959. Effect of ultrasonic waves on concentration gradients, J. Acoust. Soc. Am., 31(10):1372–1376.

Pons et al., 1999. Thermodynamic based comprision of sorption system for cooling and heat pumpiny, Int. J. Refrig., 22 (1): 5-17.

Pons, M. and Poyelle, F. 1999. Adsorptive machines with advances cycles for heat pumping or cooling applications, Int. J. Refrig., 22 (1): 22-37.

Pridasawas, W. 2006. Solar-driven refrigeration systems with focus on the ejector cycle.

Qu, T.F. Wang, R. Z. and Wang, W. 2001. Study heat and mass recovery in adsorption refrigeration cycles, Applied Thermal Engineering, 21:439-452.

Rege, S.L. Yang, R.T. and Cain, C.A. 1998. Desorption by ultrasound: Phenol on activated carbon and polymeric resin, AIChE. J., 44(7):1519–1528.

Ruthrenss, D.M. 1984. Principle of adsorption and desorption process, New York: Wiley- Interscience.

Sangtianchai, K. 2009. Analysis of Adsorption Cooling Using Lumped Parameter Model and One Dimension Model, Master Engineering, Chiang Mai University, Chiang Mai, Thailand.

Suslick, K.S. 2008. Executive summary: the chemical and physical effects of ultrasound, http://www.scs.uiuc.edu/suslick/execsummsono.html (Dec.23, 2008).

Schueller, B.S. and Yang, R.T. 2001. Ultrasound enhanced adsorption and desorption of phenol on activated carbon and polymeric resin, Ind. Eng. Chem. Res., 40(22): 4912–4918.

Tamainot-Telto, Z. and Critoph, R.E. 2003. Advance solid sorption air conditioning modules using monolithic carbon-ammonia pair, Apply Thermal Engineering, 23(6): 659-74.

Tiansuwan, J. Kiatsiriroat, T. and Hirunlabh, J. 1995. Activated Carbon-Ethanol: An Alternative Working Substance for Adsorption Cooling System, Journal Energy Heat and Mass Transfer, 17: 65-73.

Tiansuwan, J. Hirunlabh, J. and Kiatsiriroat, T. 1998. Mathematical Model of Activated Carbon-Ethanol Refrigerator, Thammasat International Journal of Science, 3:102-116.

Wongsuwan, W. Ritthong, W. Nuntaphan, A. and Kiatsiriroat, T. 2011. Performance analysis of a modular adsorption cooling system having sonic vibration at evaporator, ASCE's Journal of Energy Engineering, 137(2): 99-107.

Wang, D.C. and Zhang, J.P. 2009. Design and performance prediction of an adsorption heat pump with multi-cooling tubes, Energy Conversation and Management, 50(5):1157-1162.

Wang, R.Z. Wu, J.Y. Xu, Y.X. and Wang, W. 2001. Performance research and improvements on heat regenerative adsorption refrigerator and heat pump, Energy Converse management, 42(2):233-249.

Wang, L.W. Wang, R.Z. Wu, J.Y. Xu, Y.X. and Wang, S.G. 2006a. Design, simulation and performance of a waste heat driven adsorption ice maker for fishing boat, Energy, 31:244-259.

Wiess, W. 2003. Comparison of system design for solar combi systems, Proceedings ISES Solar word Congress, Goteborg.

Wang, D.C. Xia, Z.Z. and Wu, J.Y. 2006b. Design and performance prediction of a novel zeolite-water adsorption air conditioner, Energy conversion and management, 47:590-610.

Wang, L.W. Wang, R.Z. Lu, Z.S. Xu, Y.X. and Wu, J.Y. 2006c. Split heat pipe type compound adsorption ice making test unit for fishing boats, International journal of refrigeration, 29:456-468.

Wu, J.Y. Wang, R.Z. and Xu, Y.X. 2002. Experimental results on operating parameters influence for an adsorption refrigerator, International Journal of Thermal and Science, 41(2):137-145.

Yang, G.Z. Xia, Z.Z. Wang, R.Z. Daou, K. Wang, D.C. Dong, Z.H. and Yang, X. 2006. Research on a compact adsorption room air conditioner, Energy Conversion and Management, 47:2167-2177.

Yaws, C.L. 1992. Thermodynamic and physical property data, Gulf Publishing, Texas.

Young, F.R. 1989. Cavitation, McGraw-Hill, New York.

Zhang, G. Wang, S. and Liu, Z. 2003. Ultrasonic regeneration of granular activated carbons, Environmental Engineering and Science, 20(1):57–64.

Zhang, L.Z. 2000. Design and testing of an automobile waste heat adsorption cooling system, Apply Thermal Engineering, 20:103-114.

APPENDICES

APPENDICE A
EXPERIMENTTAL DATA

TABLE A

EXPERIMENTDATA

PERFORMANCE ANALYSIS OF A MODULAR ADSORPTION COOLING SYSTEM HAVING SONIC VIBRATION AT EVAPORATOR

Table A 1. Experimental temperature data with time for Cycle time of adsorption cooling system.

Time (min.)	$T_{w,evap\_in}$ (^{0}C)	$T_{w,evap\_out}$ (^{0}C)	T_{act_upper} (^{0}C)	T_{evap_mid} (^{0}C)
0	28.10	26.30	31.80	26.30
60	28.00	26.20	37.40	26.40
120	27.80	26.10	43.00	26.40
180	27.70	26.10	48.60	26.40
240	27.60	26.00	53.50	26.40
300	27.50	26.00	58.40	26.40
360	27.40	25.90	57.50	26.70
420	27.30	25.90	60.30	26.60
480	27.20	25.80	63.00	26.60
540	27.10	25.70	65.50	26.50
600	27.00	25.70	67.70	26.50
660	26.90	25.70	69.70	26.40
720	26.90	25.60	72.50	26.40
780	26.60	25.40	74.10	26.30
840	26.70	25.50	75.50	26.30
900	26.50	25.40	76.80	26.20
960	26.50	25.50	78.00	26.20
1020	26.40	25.40	78.80	26.10
1080	26.30	25.40	79.60	26.00
1140	26.30	26.10	80.10	26.00
1200	26.30	26.30	75.40	26.10
1260	27.20	26.60	64.90	26.30
1320	27.50	26.70	56.50	26.40
1380	27.90	26.90	50.20	26.50
1440	28.00	26.90	45.60	26.60
1500	28.10	27.50	42.20	26.80
1560	28.20	25.70	39.60	26.90
1620	28.20	23.90	41.80	24.20
1680	28.30	22.30	46.00	22.70
1740	28.20	21.30	48.40	21.70
1800	28.40	20.20	50.90	20.50
1860	28.40	19.80	51.70	20.00
1920	28.40	19.90	51.20	20.00
1980	28.50	20.30	49.90	20.40
2040	28.50	20.80	48.40	20.90
2100	28.50	21.20	46.80	21.30
2160	28.50	21.70	45.10	21.80
2220	28.50	22.20	43.40	22.40
2280	28.50	22.50	42.00	22.60

Table A 1. Experimental temperature data with time for Cycle time of adsorption cooling system. (Continuous)

Time (min.)	$T_{w,evap\_in}$ (^0C)	$T_{w,evap\_out}$ (^0C)	T_{act_upper} (^0C)	T_{evap_mid} (^0C)
2340	28.50	22.90	40.50	23.00
2400	28.40	23.30	39.10	23.30
2460	28.40	23.80	37.90	23.60
2520	28.40	24.00	36.90	24.00
2580	28.50	24.50	35.90	24.30
2640	28.40	24.60	35.10	24.30
2700	28.40	25.10	34.40	24.70
2760	28.30	25.30	33.70	24.90
2820	28.30	25.60	33.10	25.20
2880	28.30	25.70	32.60	25.20
2940	28.30	25.90	32.20	25.40

Table A 2. Experimental temperature with time data for Cool down time of activated carbon at various cooling methods.

Time (min)	T_{hp} (^{0}C)	T_{w} (^{0}C)	T_{w+hp} (^{0}C)	Time (min)	T_{hp} (^{0}C)
0	80.00	80.00	80.00	4800	32.00
120	78.50	73.00	71.00	4920	31.60
240	77.30	65.00	62.00	5040	31.20
360	75.40	59.00	56.00	5160	30.92
480	72.27	53.00	49.00	5280	30.76
600	69.00	49.00	45.00	5400	30.60
720	65.80	45.00	42.00	5520	30.36
840	62.60	42.00	39.00	5640	30.12
960	60.00	39.20	37.00		
1080	58.20	38.00	35.00		
1200	56.40	36.20	34.00		
1320	54.80	35.00	33.00		
1440	53.00	33.80	32.00		
1560	52.00	32.60	31.00		
1680	50.00	32.00	30.50		
1800	48.50	31.60	30.00		
1920	47.20	31.20			
2040	45.20	31.00			
2160	44.20	30.80			
2280	43.80	30.60			
2400	42.60	30.20			
2520	42.00				
2640	41.00				
2760	40.00				
2880	39.00				
3000	38.00				
3120	37.60				
3240	36.80				
3360	36.30				
3480	36.20				
3600	36.00				
3720	35.40				
3840	34.80				
3960	34.40				
4080	34.20				
4200	34.00				
4320	33.40				
4440	32.80				
4560	32.40				
4680	32.20				

Table A 3. Experimental temperature with time data for Temperature profiles of adsorption system with time.

			0 kHz	8 kHz	10 kHz	14 kHz
Time (min.)	$T_{w,evap\_in}$ (^{0}C)	$T_{w,evap\_out}$ (^{0}C)	T_{evap} (^{0}C)	T_{evap} (^{0}C)	T_{evap} (^{0}C)	T_{evap} (^{0}C)
0	28.10	26.30	26.30	26.10	25.80	25.70
120	27.80	26.10	26.40	26.10	25.80	25.70
240	27.60	26.00	26.40	26.10	26.00	25.80
360	27.40	25.90	26.70	26.70	26.30	26.40
480	27.20	25.80	26.60	26.50	26.10	26.10
600	27.00	25.70	26.50	26.60	26.10	26.20
720	26.90	25.60	26.40	26.60	26.10	26.30
840	26.70	25.50	26.30	26.50	26.10	26.20
960	26.50	25.50	26.20	26.50	26.00	26.20
1080	26.30	25.40	26.00	26.40	26.00	26.20
1200	26.30	26.30	26.10	26.30	26.50	26.60
1320	27.50	26.70	26.40	26.20	26.60	26.70
1440	28.00	26.90	26.60	26.40	26.70	26.70
1560	28.20	25.70	26.90	26.30	20.90	17.80
1680	28.30	22.30	22.70	17.10	17.70	18.10
1800	28.40	20.20	20.50	18.00	18.20	19.40
1920	28.40	19.90	20.00	19.30	19.40	20.70
2040	28.50	20.80	20.90	20.20	20.50	22.00
2160	28.50	21.70	21.80	21.50	21.50	23.00
2280	28.50	22.50	22.60	22.50	22.40	24.00
2400	28.40	23.30	23.30	23.20	23.50	24.80
2520	28.40	24.00	24.00	24.10	24.20	25.50
2640	28.40	24.60	24.30	24.70	24.80	
2760	28.30	25.30	24.90	25.30		
2880	28.30	25.70	25.20			
3000	28.20	26.00	25.60			

Table A 4. Experimental temperature with time data in case of sonic wave vibration at evaporator (Condition: $T_{ads}/T_{cw\_cond}/T_{valve}$: 90/20/70).

Time (s)	T_{w_i} (^{0}C)	T_{w_e} (^{0}C)	T_{b_exp} (^{0}C)	$T_{wo,cd}$ (^{0}C)	$T_{wi,cd}$ (^{0}C)	T_{ev} (^{0}C)	T_{cw_evi} (^{0}C)
0	27.1	27.6	26.7	23.8	23.7	23.7	23.6
30	27.0	27.6	26.8	23.7	23.7	23.8	23.5
60	43.8	27.6	26.7	23.8	23.7	23.9	23.5
90	81.1	68.8	34.5	23.8	23.7	23.8	23.5
120	85.4	82.3	46.0	23.8	23.8	23.9	23.6
150	86.0	84.3	54.7	23.8	23.9	23.9	23.5
180	86.3	85.1	61.2	23.9	23.9	23.9	23.5
210	86.5	85.5	66.3	23.9	23.8	23.9	23.6
240	86.6	85.9	70.2	26.5	27.5	24.5	23.7
270	86.7	85.9	69.2	28.6	28.3	26.7	23.7
300	87.0	86.1	70.6	28.3	28.2	26.4	23.7
330	87.0	86.2	72.4	28.1	28.0	26.2	23.7
360	87.0	86.5	74.0	28.1	28.1	26.0	23.7
390	87.2	86.5	75.5	28.1	28.1	25.8	23.7
420	87.3	86.8	77.0	28.1	28.1	25.8	23.7
450	87.6	87.2	78.9	28.0	28.1	25.6	23.7
480	87.9	87.6	80.6	28.0	28.0	25.6	23.8
510	88.3	87.4	81.8	28.0	28.0	25.5	23.8
540	88.6	88.3	82.9	28.0	28.1	25.5	23.9
570	88.8	88.5	83.9	28.1	28.1	25.4	24.0
600	89.1	88.9	84.6	28.1	28.2	25.4	24.1
630	89.4	89.2	85.3	28.1	28.2	25.5	24.1
660	89.6	89.3	85.8	28.1	28.1	25.4	24.2
690	90.0	89.8	86.4	28.1	28.1	25.4	24.3
720	90.2	90.0	86.9	28.1	28.1	25.4	24.3
750	90.3	90.1	87.2	28.0	28.1	25.5	24.3
780	90.5	90.3	87.7	28.1	28.1	25.5	24.3
810	90.9	90.7	88.1	28.0	28.1	25.5	24.2
840	91.1	90.9	88.4	28.0	28.1	25.5	24.2
870	91.3	91.2	88.8	27.9	28.0	25.5	24.2
900	91.7	91.5	89.1	27.9	28.1	25.5	24.1
930	91.8	91.7	89.4	28.0	28.1	25.6	24.3
960	92.2	91.9	89.7	28.1	28.1	25.5	24.2
990	92.2	92.1	89.9	28.1	28.1	25.5	24.4
1020	91.5	91.4	90.4	28.4	28.1	25.7	24.5
1050	28.6	42.6	55.4	28.7	27.6	25.9	24.6
1080	28.7	31.8	41.8	29.1	27.4	25.9	24.7
1110	27.6	29.2	37.4	29.4	27.2	25.9	24.5
1140	27.9	29.0	35.9	29.7	27.2	26.0	25.9
1170	28.0	29.1	35.1	28.8	26.5	24.6	25.9

Table A 4. Experimental temperature with time data in case of sonic wave vibration at evaporator (Condition: $T_{ads}/T_{cw\_cond}/T_{valve}$: 90/20/70). (Continuous)

Time (s)	T_{w_i} (^{0}C)	T_{w_e} (^{0}C)	T_{b_exp} (^{0}C)	$T_{wo,cd}$ (^{0}C)	$T_{wi,cd}$ (^{0}C)	T_{ev} (^{0}C)	T_{cw_evi} (^{0}C)
1200	27.8	28.9	37.4	27.6	24.5	22.2	25.7
1230	27.6	28.5	36.4	26.5	22.8	20.8	25.7
1260	27.6	28.4	34.9	25.6	21.8	20.2	25.8
1290	28.0	28.5	34.4	24.9	21.4	20.0	25.9
1320	27.5	28.1	33.0	24.0	20.6	19.6	25.4
1350	27.5	27.8	31.9	23.4	20.4	19.8	25.3
1380	28.4	28.7	31.9	23.1	20.7	20.3	25.1
1410	28.2	28.4	30.9	22.9	21.0	20.7	24.7
1440	28.4	28.4	30.1	22.7	21.1	21.0	24.4
1470	28.1	28.2	29.5	22.3	21.0	21.5	24.1
1500	27.6	27.7	28.5	22.3	21.1	21.6	23.9
1530	28.3	28.4	29.1	22.3	21.4	21.8	24.2
1560	28.0	28.0	28.4	22.4	21.6	22.3	24.2
1590	28.0	28.0	28.1	22.5	21.8	22.5	24.0
1620	28.2	28.2	28.2	22.8	22.3	22.7	23.8
1650	27.7	27.7	27.5	23.0	22.5	22.8	23.3
1680	27.8	27.7	27.5	23.5	23.1	23.1	23.4

TABLE B

EXPERIMENT DATA

PERFORMANCE ANALYSIS OF A MODULAR ADSORPTION COOLING SYSTEM WITH SONIC VIBRATION IN THE ADSORBER

Table B 1. Experimental temperature with time data for Temperature profiles of the adsorption system.

	Time (s)	T_{ads} (^{0}C)	$T_{w,evap\_in}$ (^{0}C)	$T_{w,evap\_out}$ (^{0}C)	T_{evap} (^{0}C)
0 kHz	0	28.00	19.40	30.40	18.90
	30	27.90	19.40	29.80	19.10
	60	27.80	19.40	29.90	19.20
	90	27.90	19.60	29.40	19.40
	120	42.50	19.60	29.40	19.70
	150	62.30	19.50	31.00	19.80
	180	69.40	19.50	29.00	19.90
	210	71.50	19.60	30.50	20.70
	240	73.10	19.70	30.90	21.20
	270	75.10	19.70	29.70	21.60
	300	76.80	19.80	29.40	21.90
	330	78.20	19.80	29.70	22.00
	360	79.50	19.90	31.10	22.20
	390	80.80	19.90	29.30	22.30
	420	81.80	20.00	30.90	22.20
	450	82.80	20.00	30.60	22.30
	480	83.70	20.00	31.10	22.30
	510	85.20	20.20	31.10	22.30
	540	86.50	20.30	29.40	22.30
	570	87.60	20.40	30.40	22.40
	600	88.60	20.50	30.50	22.50
	630	89.40	20.70	29.30	22.60
	660	90.20	21.00	29.40	22.60
	690	90.80	21.20	30.70	22.70
	720	81.60	21.40	29.90	22.70
	750	56.90	21.70	30.00	22.90
	780	45.80	21.70	30.30	23.00
	810	39.50	24.00	30.40	22.90
	840	40.40	23.60	29.90	22.90
	870	42.70	20.40	29.80	19.90
	900	39.50	17.30	29.90	18.40
	930	37.20	16.20	30.00	17.30
	960	35.30	16.20	30.80	16.30
	990	34.00	16.50	29.60	15.80
	1020	32.90	16.70	30.50	15.60
	1050	32.20	17.00	29.70	15.70
	1080	31.40	17.40	29.30	15.90
	1110	30.80	17.70	29.70	16.20
	1140	30.40	18.10	30.40	16.50

Table B 1. Experimental temperature with time data for Temperature profiles of the adsorption system. (Continuous)

	Time (s)	T_{ads} (^0C)	$T_{w,evap\_in}$ (^0C)	$T_{w,evap\_out}$ (^0C)	T_{evap} (^0C)
	1170	30.00	18.30	30.60	16.80
	1200	29.70	18.60	29.90	17.10
	1230	29.40	19.00	30.60	17.40
	1260	29.00	19.60	30.90	17.80
	1290	28.90	20.00	31.20	18.20
	1320	28.70	19.80	29.90	18.70
	1350	28.60	19.10	30.20	18.90
	1380	28.40	18.00	31.20	18.90
8 kHz	1410	27.00	23.80	31.10	24.30
	1440	27.00	23.80	30.40	24.40
	1470	27.00	23.80	31.10	24.40
	1500	27.00	23.80	30.80	24.40
	1530	27.00	23.80	29.10	24.40
	1560	27.10	23.90	30.10	24.50
	1590	39.30	23.80	30.50	24.50
	1620	58.70	23.90	31.00	24.50
	1650	66.20	23.90	31.10	24.50
	1680	70.30	23.90	30.50	25.10
	1710	70.60	23.90	30.50	25.80
	1740	72.40	23.90	30.40	26.00
	1770	74.20	24.00	30.60	26.20
	1800	75.80	24.00	29.90	26.50
	1830	77.20	24.10	30.80	26.50
	1860	79.30	24.00	29.70	26.60
	1890	81.50	24.10	29.40	26.50
	1920	83.50	24.10	32.00	26.40
	1950	84.90	24.20	29.20	26.20
	1980	86.20	24.30	30.30	26.20
	2010	87.20	24.30	31.20	26.10
	2040	88.10	24.30	31.00	26.10
	2070	89.00	24.40	31.30	26.10
	2100	89.70	24.40	31.30	26.10
	2130	90.50	24.40	31.40	26.10
	2160	70.80	24.50	30.40	26.50
	2190	51.60	24.50	30.70	26.70
	2220	42.80	24.70	30.60	26.80
	2250	38.40	26.50	29.90	26.60
	2280	37.80	26.40	30.50	26.10
	2310	42.90	26.30	29.70	21.70
	2340	40.00	26.20	29.80	20.00

Table B 1. Experimental temperature with time data for Temperature profiles of the adsorption system. (Continuous)

	Time (s)	T_{ads} (^{0}C)	$T_{w,evap\_in}$ (^{0}C)	$T_{w,evap\_out}$ (^{0}C)	T_{evap} (^{0}C)
	2400	36.10	25.80	29.60	19.10
	2430	34.70	25.00	30.10	19.20
	2460	33.60	24.20	30.60	19.60
	2490	32.60	23.40	31.50	19.30
	2520	31.50	22.90	31.00	19.50
	2550	31.00	22.20	30.90	19.50
	2580	30.20	21.80	29.30	19.80
	2610	29.80	21.30	31.70	19.90
	2640	29.40	20.90	30.40	20.00
	2670	29.10	20.50	30.30	20.20
	2700	28.70	20.40	29.60	20.20
	2730	28.50	20.30	30.80	20.50
	2760	28.30	20.50	30.00	20.80
10 kHz	2790	28.20	17.70	30.10	18.90
	2820	28.20	17.80	29.90	18.90
	2850	28.10	17.90	30.40	19.10
	2880	28.20	18.00	30.90	19.10
	2910	28.10	18.10	29.60	19.20
	2940	28.20	18.10	29.70	19.30
	2970	28.10	18.30	29.40	19.30
	3000	28.20	18.40	30.80	19.40
	3030	28.10	18.50	30.90	19.50
	3060	33.70	18.60	30.10	19.50
	3090	55.80	18.70	31.00	19.60
	3120	70.30	18.70	30.80	19.60
	3150	71.10	18.80	29.10	19.80
	3180	74.40	19.00	30.20	20.10
	3210	73.60	19.20	31.20	21.30
	3240	76.30	19.30	29.10	21.80
	3270	78.90	19.60	30.40	22.10
	3300	81.20	19.80	29.10	22.20
	3330	83.00	20.00	31.00	22.20
	3360	84.60	20.20	29.80	22.20
	3390	86.00	20.30	31.00	22.30
	3420	87.10	20.50	30.40	22.30
	3450	88.20	20.50	31.20	22.40
	3480	89.00	20.50	29.60	22.40
	3510	89.80	20.60	30.30	22.50
	3540	90.50	20.70	30.80	22.50
	3570	69.90	21.20	30.40	22.90

Table B 1. Experimental temperature with time data for Temperature profiles of the adsorption system. (Continuous)

	Time (s)	T_{ads} (^{0}C)	$T_{w,evap\_in}$ (^{0}C)	$T_{w,evap\_out}$ (^{0}C)	T_{evap} (^{o}C)
	3600	52.70	21.30	31.20	23.10
	3630	43.60	21.40	30.30	23.30
	3660	38.60	22.80	31.00	23.10
	3690	39.10	21.90	30.70	22.70
	3720	42.00	19.40	30.90	19.10
	3750	39.30	18.60	30.80	17.90
	3780	37.30	18.70	29.80	17.40
	3810	35.80	18.90	30.00	17.30
	3840	34.50	19.50	30.10	17.30
	3870	33.60	19.60	31.10	17.40
	3900	32.70	19.30	30.40	17.80
	3930	32.00	18.30	30.20	18.10
	3960	31.10	17.00	29.90	18.00
	3990	30.40	16.50	30.20	17.60
	4020	29.90	16.60	31.20	17.20
	4050	29.50	16.90	29.60	17.20
	4080	29.00	17.40	31.30	17.20
	4110	28.80	18.00	31.40	17.50
	4140	28.60	18.40	29.90	17.90
	4170	28.40	18.90	31.10	18.40
14 kHz	4200	26.80	21.00	29.80	20.70
	4230	26.80	21.00	30.50	20.60
	4260	26.80	21.00	31.10	20.70
	4290	26.70	21.10	31.30	20.70
	4320	26.70	21.10	29.50	20.80
	4350	26.70	21.10	29.20	20.80
	4380	26.70	21.10	30.10	20.80
	4410	26.70	21.20	30.80	20.90
	4440	26.60	21.30	30.60	21.10
	4470	26.60	21.30	30.30	21.20
	4500	26.70	21.30	30.20	21.20
	4530	26.60	21.40	30.60	21.30
	4560	26.60	21.30	31.10	21.30
	4590	26.70	21.40	29.90	21.40
	4620	26.70	21.50	31.20	21.40
	4650	26.70	21.50	30.40	21.60
	4680	28.30	21.70	30.10	21.70
	4710	63.00	21.80	31.40	21.90
	4740	70.70	21.90	29.80	23.30
	4770	74.60	21.90	30.80	24.10

Table B 1. Experimental temperature with time data for Temperature profiles of the adsorption system. (Continuous)

Time (s)	T_{ads} (^{0}C)	$T_{w,evap\_in}$ (^{0}C)	$T_{w,evap\_out}$ (^{0}C)	T_{evap} (^{0}C)
4800	78.00	22.10	30.10	24.20
4830	80.40	22.10	29.60	24.50
4860	82.20	22.20	30.80	24.50
4890	83.70	22.30	31.30	24.40
4920	85.00	22.40	30.10	24.40
4950	86.30	22.50	30.40	24.40
4980	87.20	22.60	31.10	24.40
5010	88.10	22.60	30.60	24.30
5040	89.00	22.70	30.10	24.30
5070	89.70	22.80	31.00	24.30
5100	90.40	22.90	29.80	24.50
5130	53.60	23.30	31.30	25.50
5160	40.50	25.30	29.60	26.10
5190	35.50	19.10	30.60	24.70
5220	41.90	18.50	29.30	19.00
5250	38.00	18.70	29.40	17.30
5280	35.40	19.10	29.60	16.90
5310	33.60	19.70	31.00	17.00
5340	32.30	19.90	31.90	18.10
5370	31.20	19.40	29.60	18.90
5400	30.30	18.00	30.10	19.40
5430	29.40	17.20	29.70	18.90
5460	28.70	17.30	30.40	18.30
5490	28.20	17.80	31.30	18.30
5520	28.10	18.30	31.30	18.90
5550	27.90	18.80	30.20	19.30
5580	27.70	19.50	30.50	19.60

Table B 2. Experimental temperature with time data in case of sonic wave vibration at adsorber (Condition: $T_{ads}/T_{cw\_cond}/T_{valve}$: 90/20/70).

Time (s)	T_{w_i} (^{0}C)	T_{w_e} (^{0}C)	T_{b_exp} (^{0}C)	$T_{wo,cd}$ (^{0}C)	$T_{wi,cd}$ (^{0}C)	T_{ev} (^{0}C)	T_{cw_evi} (^{0}C)
0	25.8	27.9	26.0	24.0	23.8	23.3	23.0
30	66.7	43.8	28.4	24.0	23.8	23.3	23.0
60	83.2	78.7	49.6	24.2	24.0	23.3	23.2
90	85.1	83.0	60.9	24.2	24.0	23.3	23.2
120	85.9	84.4	67.0	24.2	24.0	23.4	23.3
150	86.3	85.2	70.8	24.1	23.9	23.4	23.2
180	86.6	85.6	73.4	24.1	23.9	23.4	23.2
210	86.9	85.8	73.5	28.9	28.5	23.9	23.2
240	87.1	86.1	74.0	28.7	28.6	24.3	23.3
270	87.2	86.3	75.5	28.6	28.5	24.5	23.3
300	87.2	86.5	76.6	28.4	28.3	24.5	23.3
330	87.2	86.5	77.6	28.2	28.1	24.5	23.4
360	87.5	86.9	78.7	28.2	28.1	24.5	23.4
390	87.5	86.9	79.4	28.1	28.0	24.5	23.4
420	87.8	87.2	80.2	28.1	28.1	24.5	23.4
450	87.9	86.9	81.0	28.1	28.1	24.5	23.3
480	88.1	87.6	81.9	28.1	28.1	24.5	23.3
510	88.0	87.6	82.2	28.0	28.1	24.5	23.3
540	88.3	87.9	82.8	28.0	28.1	24.5	23.3
570	88.6	88.1	83.4	27.9	28.0	24.6	23.4
600	88.8	88.4	83.8	27.7	27.8	24.5	23.3
630	88.8	88.3	84.1	27.7	27.8	24.5	23.4
660	89.1	88.8	84.6	27.8	27.9	24.5	23.4
690	89.2	89.0	85.0	27.8	27.9	24.6	23.4
720	89.4	89.2	85.3	27.7	27.9	24.5	23.4
750	89.6	89.3	85.6	28.0	28.0	24.6	23.6
780	89.7	89.6	86.0	28.0	28.0	24.5	23.7
810	90.0	89.7	86.3	28.1	28.1	24.8	23.8
840	90.1	89.8	86.5	28.1	28.1	24.7	23.8
870	90.1	89.9	86.9	28.1	28.1	24.8	23.8
900	90.3	90.1	87.0	28.1	28.2	24.8	23.9
930	90.4	90.2	87.3	28.0	28.1	24.6	23.8
960	90.6	90.4	87.5	28.1	28.2	24.7	23.9
990	90.5	90.4	87.7	28.1	28.2	24.6	23.9
1020	90.9	90.7	88.0	28.1	28.2	24.7	23.9
1050	90.9	90.8	88.1	28.2	28.2	24.7	24.0
1080	91.1	90.9	88.4	28.2	28.2	24.7	24.0

Table B 2. Experimental temperature with time data in case of sonic wave vibration at adsorber (Condition: $T_{ads}/T_{cw\_cond}/T_{valve}$: 90/20/70). (Continuous)

Time (s)	T_{w_i} (^0C)	T_{w_e} (^0C)	T_{b_exp} (^0C)	$T_{wo,cd}$ (^0C)	$T_{wi,cd}$ (^0C)	T_{ev} (^0C)	T_{cw_evi} (^0C)
1110	91.2	90.9	88.6	28.1	28.3	24.7	23.9
1140	91.3	91.1	88.8	28.2	28.3	24.7	23.9
1170	91.4	91.3	89.1	28.1	28.2	24.7	23.9
1200	91.7	91.6	89.3	28.1	28.2	24.7	23.8
1230	92.0	92.0	89.8	28.1	28.3	24.7	23.9
1260	92.3	92.1	90.1	28.1	28.2	24.8	24.0
1290	91.4	91.7	90.2	28.4	28.1	25.0	24.0
1320	28.1	37.4	70.5	28.8	27.7	25.0	24.1
1350	28.7	31.3	53.4	29.3	27.5	25.2	24.5
1380	27.8	29.4	44.2	29.6	27.4	25.3	24.3
1410	28.3	29.1	38.8	29.6	27.4	25.3	25.4
1440	28.3	29.0	36.1	29.2	27.3	25.2	25.4
1470	28.1	28.7	38.3	28.2	25.7	23.6	24.2
1500	28.7	30.0	41.7	26.4	22.7	19.9	23.8
1530	27.8	28.7	39.2	25.0	21.2	19.5	23.6
1560	28.2	29.0	37.8	24.0	20.9	20.1	23.9
1590	28.1	28.8	36.2	23.4	21.1	20.5	24.2
1620	28.6	29.2	34.5	23.1	21.4	21.1	24.0
1650	27.8	28.3	33.1	23.0	21.6	21.6	23.2
1680	27.8	28.1	32.1	22.8	21.5	21.5	21.9
1710	28.3	28.6	31.2	22.7	21.5	21.3	21.3
1740	28.3	28.5	30.5	22.7	21.3	21.0	21.3
1770	29.0	29.2	29.9	22.5	21.2	20.8	21.6
1800	27.7	27.7	29.2	22.2	21.0	20.9	21.7
1830	28.4	28.4	29.1	22.2	21.1	21.1	22.2
1860	28.5	28.5	28.9	22.1	21.2	21.3	22.5

APPENDICE B

LIST OF PICTURES

EXPERIMWENT TOOLS

EXPERIMENT TOOLS

The TASK data logger 16 channel set of K-type thermocouples having ± 0.01 ^{0}C accuracy and recorded every 30 second.

Figure 1. The TASK data logger.

The mass of activated carbon in adsorber is measured by a weighing machine having ± 0.1 ^{0}C g accuracy.

Figure 2. Weighing machine

The mass flow rate of water is measured by Rota meter having ± 0.1 LPM accuracy.

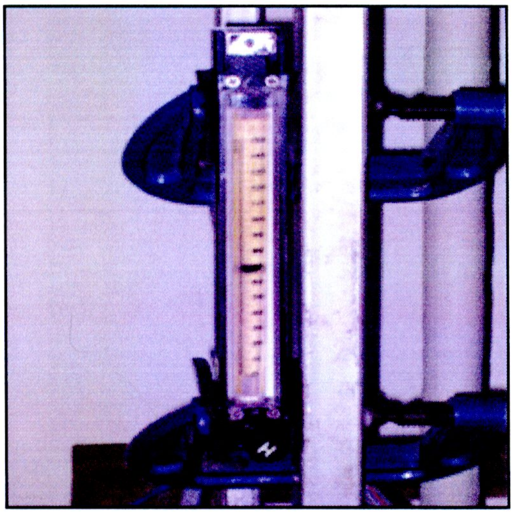

Figure 3. Rota meter

Sensor line for used temperature measurement in test unit system make from thermocouple type K product by OMEGA Corporation limited, metal compound 2 types are chromel and alumel by connection with Data logger.

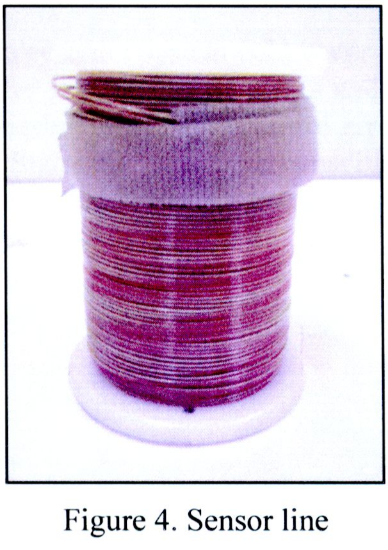

Figure 4. Sensor line

Pressure gauge for used vacuum pressure measurement inside of Adsorber, condenser and evaporator.

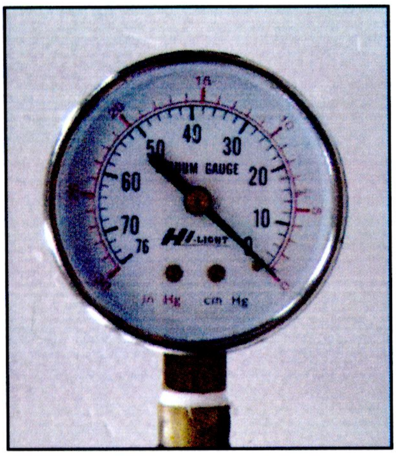

Figure 5. Pressure gauge

Heat source temperature system: system group gives the heat composes a basin gives the heat makes of , Stainless steel , 50 cm x 50 cm x 45 cm sizes , there are 112.5 L capacities by use the water is a substance works , Heater 6 1 kW amount sizes , be formed give the heat , the cabinet controls hot water temperature in a basin which , be valuable 0.4°C justices use the pump in water circulation from hot water basin for , the heat and the part due to evaporate , the speed round 3,000 rpm, 23-38.5 m height of water Tank and 5 Amp electric current by volume flow rate 30-80 L/min gives the heat shows in Figure 6.

Heat sink temperature system : system cold water group used refrigerant vapor compressor , by use the water is a substance works and there is the cabinet control cold water temperature in a basin , which able control give stable at 25°C to 2°C basin coldness justices make from Stainless steel , 98 L capacities are which , pack cold coil in a basin , the pump circulates the water from cold water basin for takes part heat condenses , there is the speed round 3,000 rpm, 15-33 m height of water Tank and 5.5 Amp electric currents by volume flow rate 20-100 L/min of system cold water capacities shows in Figure 7.

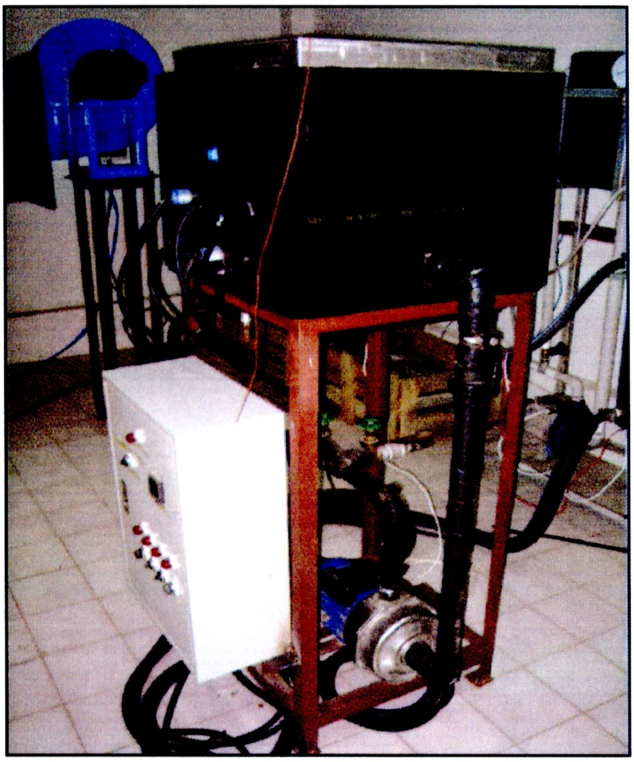

Figure 6. Heat source temperature system

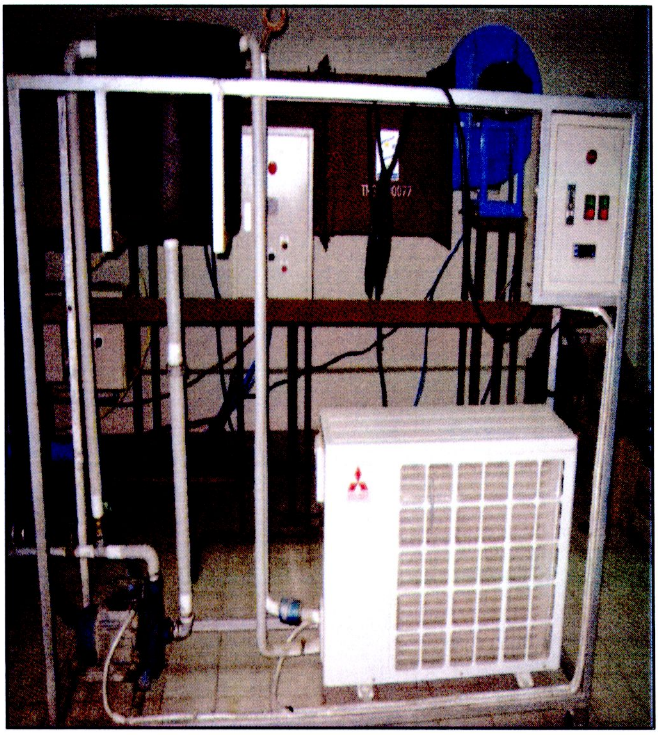

Figure 7. Heat sink temperature system

Sonic wave generator is composing 2 parts: (1) sonic wave frequency range control and (2) Head source of sonic wave by frequency value between 8-14 kHz.

Figure 8. Sonic wave generator set

APPENDICE C

LIST OF PUBLICATIONS

1. International Publications

1.1 Performance analysis of a modular adsorption cooling system having sonic vibration at evaporator. Journal of Energy Engineering, vol. 137, No. 2, June 1, 2011.

1.2 Performance analysis of a modular adsorption cooling system with sonic vibration in the adsorber. Journal of Experiment Heat Transfer, 10 May 2011, (Article inpress).

1.3 Performance Analysis of Thermosyphon Assisted Adsorption Cooling System. World Renewable Energy Congress 2009-ASIA. The 3rd International Conference on "Sustainable Energy and Environment (SEE 2009)", 18-23 May 2009, Bangkok, Thailand.

1.4 Performance study on the consolidated adsorbent bed of activated carbon-methanol adsorption cooling system. International Conference on Green and Sustainable Innovation (ICGSI) 2009, 2-4 December 2009, Chiang Rai, Thailand.

International Publications

1.1 Performance analysis of a modular adsorption cooling system having sonic vibration at evaporator. Journal of Energy Engineering, vol. 137, No. 2, June 1, 2011.

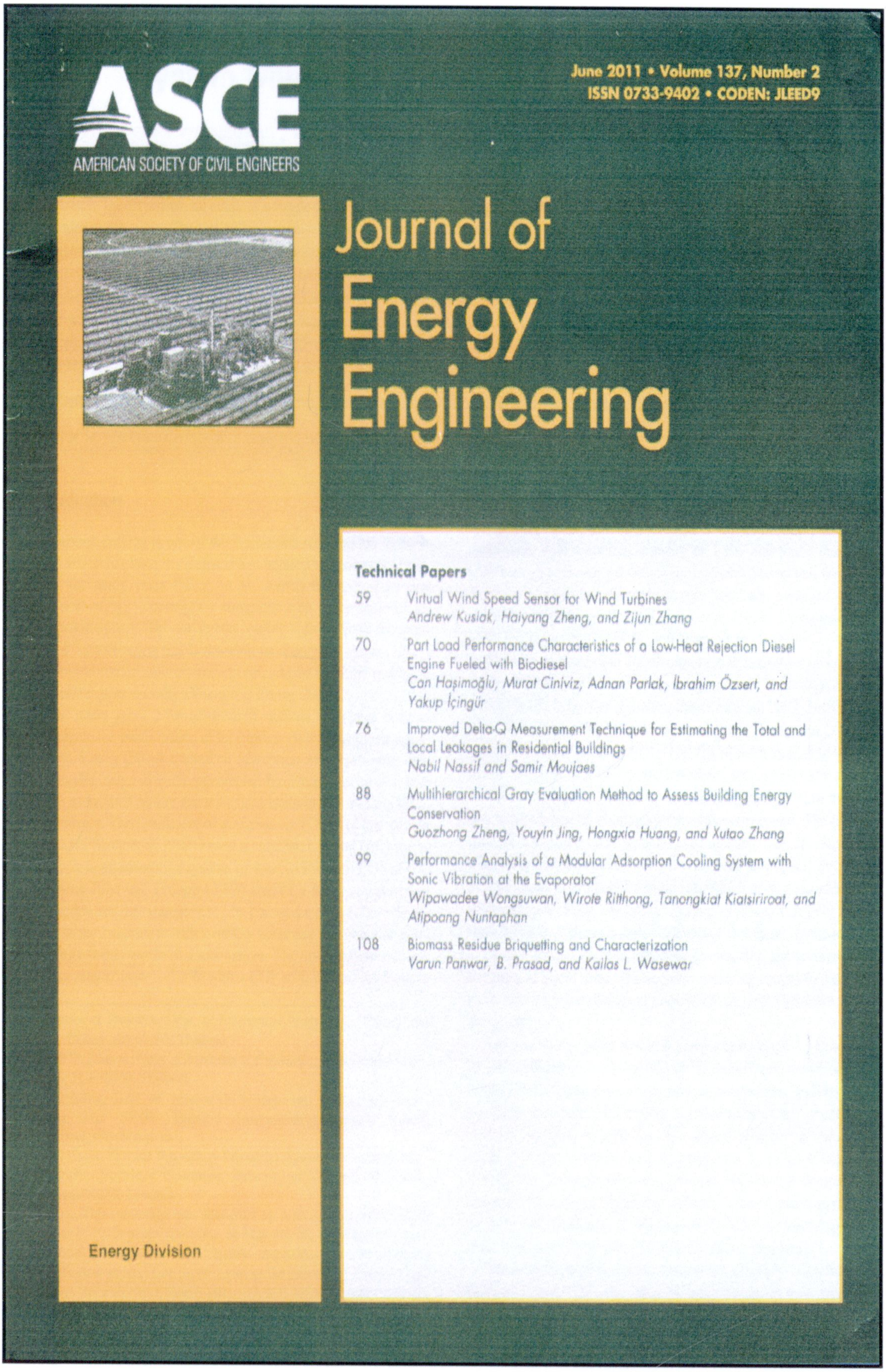

ASCE
AMERICAN SOCIETY OF CIVIL ENGINEERS

June 2011 • Volume 137, Number 2
ISSN 0733-9402 • CODEN: JLEED9

Journal of Energy Engineering

Technical Papers

Energy Division

Performance Analysis of a Modular Adsorption Cooling System with Sonic Vibration at the Evaporator

Wipawadee Wongsuwan[1]; Wirote Ritthong[2]; Tanongkiat Kiatsiriroat[3]; and Atipoang Nuntaphan[4]

Abstract: The experimental study of a single-effect modular adsorption cooling system with an activated carbon-methanol working pair is presented in this paper. The test unit is comprised of an adsorber, a condenser, and an evaporator in vertical alignment. Heating and cooling at the adsorber is by hot water at 70–90°C, whereas heating at the evaporator is performed by water at the ambient temperature. At the evaporator, a sonic wave generator enhances heat transfer for the boiling of methanol during the adsorption process. The system performance by considering the coefficient of performance (COP), specific cooling power (SCP), and volumetric cold production (VCP) is evaluated, and the sonic wave is demonstrated to reduce the evaporation time of methanol, which results in better system performances compared with the results in literature. The highest COP and SCP obtained from this system are 0.718 and 248.90 W/kg, respectively. **DOI:** 10.1061/(ASCE)EY.1943-7897.0000039.

CE Database subject headings: Performance characteristics; Adsorption; Cooling; Vibration; Evaporation.

Author keywords: Performance analysis; Adsorption cooling; Sonic wave.

Introduction

Adsorption cooling is one of the sustainable refrigeration technologies which has been investigated and applied into industrial processes for many years [Wang et al. 2006a] because of its low electrical energy consumption compared with a conventional refrigeration system. The adsorption cooling does not have the problem of crystallization that is found in an absorption system, and it has simple control, low operating cost, and no emission making it environmentally friendly (Wang and Zhang 2009).

For many years, a lot of research studiess have been done to investigate the performance of adsorption systems and their applications. Zhang (2000) studied an adsorption air-conditioning system having sorption beds regenerated by exhaust gases of a bus. This system used zeolite and water as adsorbent and working fluid, respectively. The coefficient of performance (COP) of this system was 0.38. Wang et al. (2001) used an activated carbon (AC)-methanol pair in an adsorption system, of was 3.8 kW with COP of 0.4. Tamainot-Telto and Critoph (2003) studied a modular adsorption air conditioner that was powered by hot air. Lu et al. (2004) developed an air conditioner with a zeolite-water pair that could be powered by exhaust gas from a locomotive. The cooling power of this system ranged from 3–5 kW with a COP of 0.21, and the temperature inside the cabin was 4–6°C lower than the ambient temperature. Yang et al. (2006) designed a compact adsorption air conditioner with a cooling capacity of 1 kW and found that the COP was approximately 0.446. Some mathematical models for predicting adsorption system performances have been presented, such as the reports performed by Tiansuwan et al. (1998), Leong and Liu (2004), Maggio et al. (2006), and Wang et al. (2006b).

The role of sonication on adsorption and desorption processes has been studied by several works (Rege et al. 1998; Breitbach and Bathen 2001; Schueller and Yang 2001; Li et al. 2002; Breitbach et al. 2003; Bathen 2003; Hamdaoui et al. 2003; Zhang et al. 2003), and most of these focused on the benefits of the treatment of toxic chemicals or pollutants by the adsorbent bed with concern for environmental issues. However, the use of a physical wave to enhance the adsorption cooling system was not reported. The influence of ultrasound was usually experimented and investigated within the laboratory scale. Sonic vibration propagated through a liquid forms micro bubbles in liquids, which grow and suddenly collapse and is called "cavitation" (Young 1989; Mason 1991). The wave vibration reduces bubble coalescence that increases the interfacial area for gas transfer, enhances gas transfer, and reduces the thickness of liquid films. The acoustic streaming caused by a sonic wave also improves the mass transfer coefficients (Schueller and Yang 2001).

The goal of this paper was to develop a new design for a modular activated carbon-methanol adsorption system with the adsorber, condenser, and evaporator in vertical alignment. The modular design helps to simplify fabrication, improve compactness of casing, increase flexibility to scale up, and reduce maintenance tasks. A sonic generator is attached at the evaporator to enhance boiling of methanol during the adsorption process. The calorimetric power was the input to the refrigerant in the sonicated evaporator as mentioned by Breitbach et al. (2003), in which the temperature rise and mass flow rate of the water medium could be measured.

The adsorption system performances are generally indicated by COP, SCP, and VCP. The effect of sonic waves on these performance indicators was also studied and discussed.

---

[1] Assistant Professor, Dept. of Mechanical Engineering, Chiang Mai Univ., Chiang Mai 50200, Thailand.

[2] Ph.D. Student, Dept. of Mechanical Engineering, Chiang Mai Univ., Chiang Mai 50200, Thailand.

[3] Professor, Dept. of Mechanical Engineering, Chiang Mai Univ., Chiang Mai 50200, Thailand (corresponding author). E-mail: kiatsiriroat_t@yahoo.co.th

[4] Engineer, Thermal Technology Research Laboratory, Mae Moh Training Center, Electricity Generating Authority of Thailand, Mae Moh, Lampang 52220, Thailand.

Note. This manuscript was submitted on June 3, 2010; approved on October 9, 2010; published online on May 16, 2011. Discussion period open until November 1, 2011; separate discussions must be submitted for individual papers. This paper is part of the *Journal of Energy Engineering*, Vol. 137, No. 2, June 1, 2011. ©ASCE, ISSN 0733-9402/2011/2-99–107/$25.00.

Adsorption Refrigeration Cycle

The relationship of pressure, temperature, and the concentration of working fluid in the adsorption cycle is shown as the *P-T-x* diagram in Fig. 1. The operation could be divided into four processes. A summary of the testing conditions in this study and in these four processes is presented in Table 1.

Process 1–2 is the isosteric heating process. In this process, the adsorbent temperature is increased from T_1 to T_2, and the vapor pressure of the working fluid adsorbed in the adsorbent is also increased from P_{evap} to P_{cond}.

Process 2–3 is the isobaric desorption process. The adsorbent is still heated and the temperature of the adsorbent is increased from T_2 to T_3. During this process, the working fluid is repelled from the adsorbent under a constant vapor pressure, which results in reducing the working fluid concentration in the adsorbent (from $x_{\max}$ to $x_{\min}$). During this process, the desorbed working fluid vapor is condensed in the condenser and the condensate is kept in the evaporator.

Process 3–4 is the isosteric cooling process. The adsorber is cooled to reduce its temperature from T_3 to T_4, and consequently the system pressure reduces from P_{cond} to P_{evap}.

Process 4–1 is the isobaric adsorption process. At this stage, the adsorber is continuously cooled from T_4 to T_1 at a constant pressure, whereas the working fluid condensate re-evaporates back and is re-adsorbed at the adsorber. Evaporation of methanol occurs at the evaporator, therefore, the evaporator extracts heat from its surroundings and the surrounding temperature could be reduced. The application of sound-wave vibration at the evaporator could stimulate the evaporation process, which results in faster vapor generation.

In this research, the activated carbon and methanol are used as the working pair and the following assumptions are considered:

1. The vapor of methanol is assumed to be an ideal gas;
2. The activated carbon has uniform size and homogeneous properties; and
3. All the components of the system are well-insulated.

According to the energy conservation principle, the energy input to the isosteric heating process 1–2 is primarily supplied to increase temperature of adsorber material from T_1 to T_2 as

$$Q_{1-2} = m_{\mathrm{ac}}(c_{p,\mathrm{ac}} + c_{p,\mathrm{met}} x_{\max})(T_2 - T_1) \tag{1}$$

where m_{ac} = mass of activated carbon; $x_{\max}$ = maximum concentration of methanol in activated carbon; and $c_{p,\mathrm{ac}}$ and $c_{p,\mathrm{met}}$ = specific heats of activated carbon and methanol, respectively.

In the isobaric desorption process 2–3, the methanol is repelled from the activated carbon so that the heat of adsorption equation is (Tiansuwan et al. 1998)

$$Q_{2-3} = m_{\mathrm{ac}}\left\{\left[c_{p,\mathrm{ac}} + c_{p,\mathrm{met}}\frac{(x_{\max} + x_{\min})}{2}\right](T_3 - T_2)\right\} + m_{\mathrm{ac}}[(x_{\max} - x_{\min})H_{\mathrm{des}}] \tag{2}$$

where $x_{\min}$ = minimum concentration of methanol in activated carbon and H_{des} = average heat of desorption/adsorption evaluated by the Clausius-Clapeyron equation (Critoph 1988) as

$$H_{\mathrm{des}} = \frac{R\ln\left(\frac{P_2}{P_1}\right)}{\left(\frac{1}{T_1} - \frac{1}{T_2}\right)} \tag{3}$$

Table 1. Summary of the Testing Conditions in This Study

Parameter	Value
Mass of activated carbon (mesh size 8 × 16)	0.5 kg
Volume of methanol	900 cm^3
Desorption process	
Inlet temperature of hot water	80–95°C
Mass flow rate of hot water	0.08 kg/s
Maximum temperature of activated carbon	70, 80, 90°C
Condensation process	
Inlet temperature of cooling water	5, 10, 15°C
Mass flow rate of cooling water	0.06 kg/s
Evaporation process	
Inlet temperature of water	28–35°C
Mass flow rate of cooling water	0.0018 kg/s
Frequency of sonic wave	0, 8, 10, 14 kHz
Adsorption process	
Inlet temperature of water	28–35°C
Mass flow rate of cooling water	0.035–0.045 kg/s

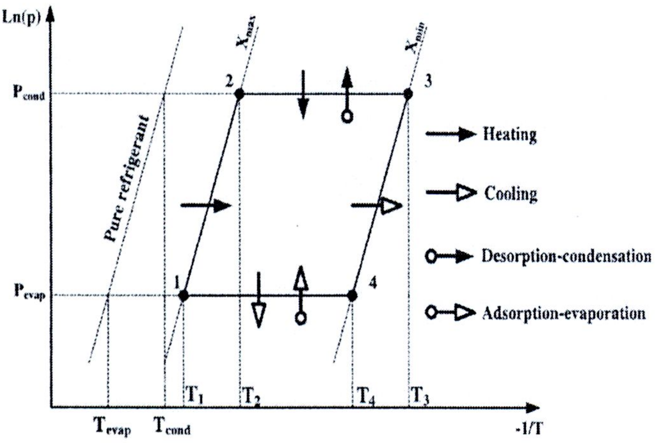

Fig. 1. *P-T-x* diagram of an adsorption cycle

where R = ideal gas constant; and P_1 and P_2 = saturated vapor pressures at state 1 and state 2, respectively. The saturated vapor pressure for methanol can be estimated from (Yaws 1992)

$$\ln P_s = 13.46853971 + (4549.236406)\left(\frac{-1}{T_s}\right) \qquad (4)$$

For the isobaric adsorption Process 4–1, the methanol is evaporated and the temperature of the adsorber reduces from T_4 to T_1. If there is no heat loss and the latent heat of vaporization (L_{met}) is assumed constant, the amount of cooling at the evaporator can be calculated from

$$Q_{\mathrm{evap}} = m_{\mathrm{ac}}(x_{\mathrm{max}} - x_{\mathrm{min}})[L_{\mathrm{met}} - c_{p,\mathrm{met}}(T_1 - T_{\mathrm{evap}})] \qquad (5)$$

During this process, a sonic generator is used to enhance the boiling of the working fluid in the evaporator in this study. The temperature difference between adsorber and evaporator is reduced, and higher heat rate at the evaporator could be expected.

The specific cooling power (SCP), the volumetric cold production (VCP), and the coefficient of performance (COP) normally determine the adsorption system performance. These parameters could be evaluated from the following three equations:

$$\mathrm{SCP} = \frac{Q_{\mathrm{evap}}}{m_{\mathrm{ac}} \times t_{\mathrm{ads}}} \qquad (6)$$

$$\mathrm{VCP} = \frac{V_{\mathrm{ads}} \times t_{\mathrm{ads}}}{Q_{\mathrm{evap}}} \qquad (7)$$

and

$$\mathrm{COP} = \frac{Q_{\mathrm{evap}}}{Q_{1-2} + Q_{2-3} + Q_{\mathrm{sonic}}} \qquad (8)$$

where t_{ads} = adsorption time; V_{ads} = volume of adsorber; and Q_{sonic} = supplied power to the sonic generator.

Inception of the Sonic Wave

The mechanical wave induced by a sonic wave generator creates variation of pressure or density. When it propagates through medium, it is attenuated by absorption, by cavitation bubbles,

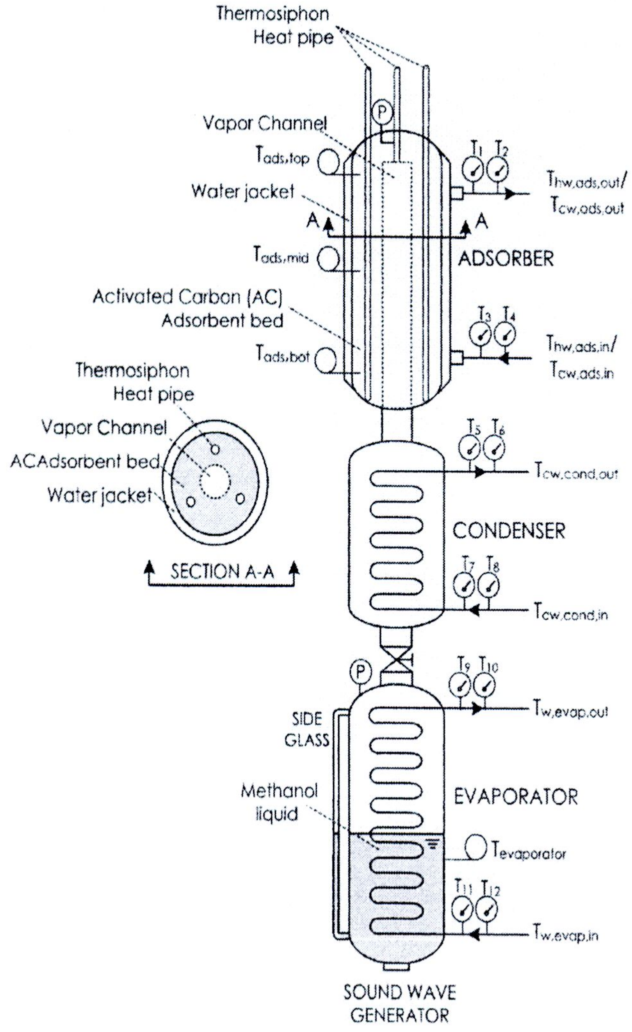

Fig. 2. Schematic sketches of the experiment apparatus

by particles, and at interfaces (Breitbach et al. 2003). The high sound intensities produce nonlinear phenomena or acoustic cavitation to exceed the liquid tensile stress. During the rarefaction cycle of sonic waves, a large negative pressure is applied to the liquid, little gas bubbles are formed during the expansion cycle of the sound-wave, and grow over one or several cycles to many times from its initial size (Juang et al. 2006). The bubbles are either stable for many cycles or transient when they grow to critical size and violently collapse intensively during the compression part of the wave. Therefore, the energy is released causing extreme thermodynamics conditions, very high temperature and pressure in the vicinity of the imploding bubbles, and large shear force in the surrounding liquid occurs (Mason 1991). As the bubble collapsed, localized areas of high temperatures led to a slight increase of the system temperature, and the localized pressures in the fluid also created high-speed microjets with high-pressure shock waves (Hamdaoui et al. 2003). The waves and the associated microdisturbances of the cavitation bubbles near the surface of the solid reduce the mass transfer boundary layer, and therefore, efficiently increase the mass transfer (Penn et al. 1959).

Experimental Setup

Fig. 2 shows the schematic sketch of the vertical solid adsorption refrigeration unit. It consists of three main parts, an adsorber, a condenser, and an evaporator. An adsorber was made of copper tubing 7.62 cm in diameter and 100 cm in height. This adsorber was filled with 0.5 kg of 8 × 16 mesh size activated carbon produced from coconut shells. The adsorber was covered with a water jacket and the whole unit was well-insulated. The height of the evaporator and condenser sections were 100 and 50 cm, respectively.

During the desorption process, hot water of 0.08 kg/s at 95°C was circulating inside the water jacket to regenerate methanol vapor at the adsorber. Then, during the cooling phase, there was cold water circulating along the water jacket.

The condenser of the adsorption system was made from copper tubing 7.62 cm in diameter and 23 cm in length. Inside, there was a copper coil 149 cm in length and 10 mm in diameter. During the condensation process, the 5–15°C and 0.06 kg/s cold water was circulating inside the copper coil.

The evaporator of the adsorption system had the same dimensions as the condenser. During the evaporation of methanol, there was water at the ambient temperature (28–35°C) circulating inside the copper coil at the flow rate of 0.0018 kg/s. To enhance vaporization process, a sonic wave generator model SUNON-DP200A (TSUS Int. Co. Ltd., Chiang Mai, Thailand) was attached at the bottom of the evaporator. The maximum frequency of this wave generator is 14 kHz.

Temperature measurements were done by a set of K-type thermocouples having ± 0.1°C accuracy and recorded by a temperature data logger model TSUS-TASK24C (TSUS Int. Co. Ltd., Chiang Mai, Thailand). The sensors were installed in the activated carbon, at the water inlet, and the outlet of the adsorber, the condenser, and the evaporator. The evaporator temperature was measured by the thermocouple at the evaporator chamber's wall. The pressures inside the adsorber and the evaporator were measured by two pressure gauges with ± 0.1 kPa accuracy. The flow rate of water was calculated by measuring the mass of the circulating water during a period of time, and the digital weighing apparatus for measuring the mass of water had ± 1 g accuracy. The methanol level inside the evaporator could be observed by a sight glass.

Results and Discussion

Thermal Behavior of Adsorption System

Fig. 3 shows the temperature profiles of the activated carbon bed (T_{ads}), the methanol in the evaporator (T_{evap}), the inlet and outlet of the circulating water at the evaporator ($T_{\mathrm{w,evap,in}}$ and $T_{\mathrm{w,evap,out}}$). Temperature evolutions from four adsorption cycles were considered. For the first cycle, during the desorption process, the adsorber was heated by hot water at approximately 90°C, and the bed temperature was increased from its initial temperature of approximately 31.8°C. The temperature increased rapidly with time, and the methanol was repelled from the activated carbon. Then, the methanol vapor flowed to the condenser where the condensation took place, and the condensate flowed downward to the evaporator. When the bed temperature reached 80°C, the desorption process stopped and the bed was cooled down by the cooling water until its temperature reached 30°C. The vapor pressure inside the adsorber dropped from approximately 180 to 21 kPa. After that, the adsorption process started and methanol vaporized back from the evaporator to the adsorber bed while it extracted heat from the circulating water, which was reducing the evaporator temperature. It was shown that the adsorber bed temperature increased because of the adsorption heat. While the cooling process was proceeding, the bed temperature then dropped to its initial temperature and the evaporator temperature slightly increased. The outlet circulating water temperature at the evaporator was seen to be slightly higher than the methanol temperature in the evaporator. The first cycle was not assisted by a sonic wave, whereas the others were assisted by a sonic wave. Obviously, the evaporator temperature with wave enhancement was lower than without wave enhancement.

Parameters Affecting Adsorption System Performance

The relevant parameters that affected the adsorption system performance were regeneration temperature, cooling water temperature at the condenser, and the cooling rate of the adsorber after the desorption process. The regeneration or heat source temperature is indicated by the inlet hot water temperature circulated through the water jacket. The mass flow rate of hot water was 0.08 kg/s and its temperature was varied at 70, 80, and 90°C. The desorbed methanol vapor flows downward to condense in a condenser. The mass flow rate and the temperature of the cooling water at the condenser are 0.06 kg/s and 10°C.

The effect of the heat source temperature on the COP, SCP, and VCP of the adsorber without sonic waves is shown in Fig. 4. The COP and SCP increased with the increasing hot water temperature, whereas the VCP decreased. The COP, SCP, and VCP were varied in the range 0.6872–0.6997, 44.30–53.25 W/kg of activated carbon, and 57.21–68.67 cm^3 of adsorber/W, respectively.

During the desorption process, the desorbed methanol vapor from the activated carbon flowed downward and condensed in the condenser. The cooling water was flowing inside the internal copper tube to remove the heat of condensation. The flow rate of the cooling water is kept constant at 0.06 kg/s and its temperature was varied at 5, 10, and 15°C. The adsorber began to be cooled down at the temperature of 80°C. The amount of condensate was measured and it was inversely proportional to the cooling water temperature.

The influence of the cooling water of the condenser on the performance of the adsorption system is illustrated in Fig. 5. COP and SCP were slightly decreased with the cooling water temperature. Inversely, the VCP was slightly increased.

A greater temperature difference between the condenser and the heat sink (or cooling water) temperature results in more condensate,

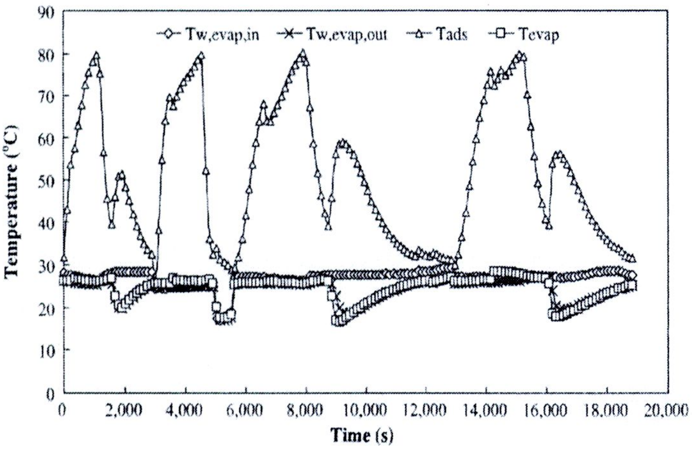

Fig. 3. Temperature profiles of the bed and the evaporator, including the evaporator circulating water

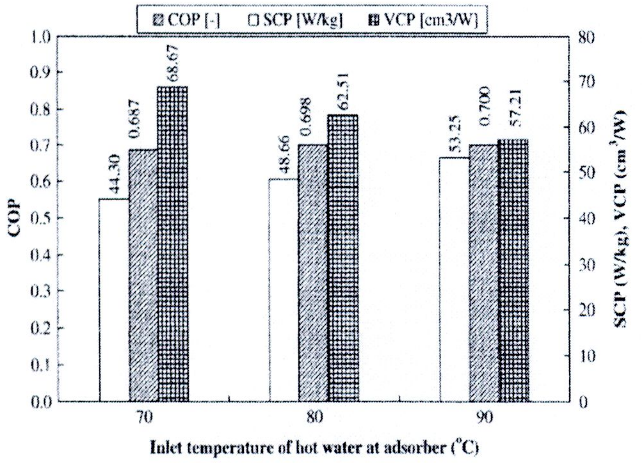

Fig. 4. Relationship of COP, SCP, and VCP with the heat source temperature without the sound wave

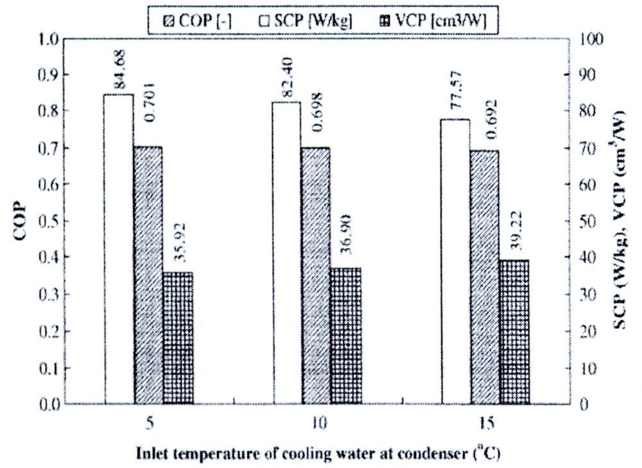

Fig. 5. Effect of cooling water temperature on system performance without the sound wave

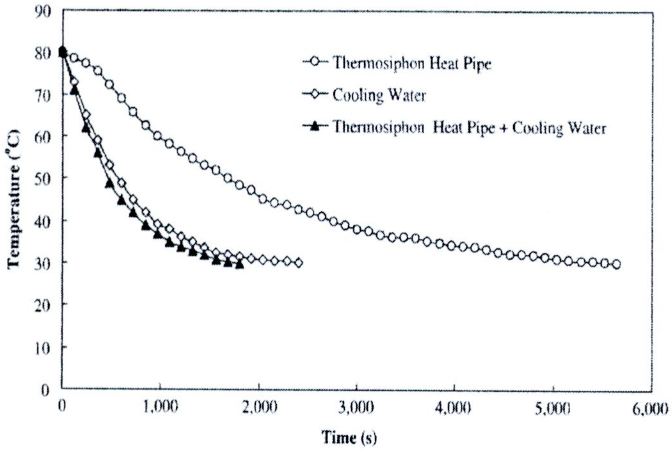

Fig. 6. Cool-down time of activated carbon at various cooling methods

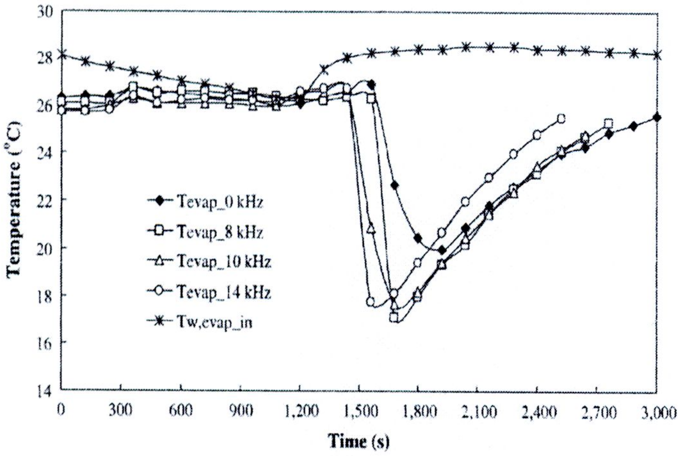

Fig. 7. Temperature profiles of the adsorption system with time

which resulted in more evaporated methanol vapor in the following adsorption phase. At 5, 10, and 15°C of cooling water temperature, the methanol volume was approximately 67.5 cm^3, 63 cm^3, and 50 cm^3, respectively. Therefore, more heat of evaporation led to higher COP and SCP.

In contrast, VCP was reduced and a greater system compactness was found during cooling. However, from 80–90°C, COP slightly increased owing to the limit of the amount of adsorbent methanol in the adsorbent bed.

During the cooling process, the activated carbon bed rejected heat to the environment by the thermosiphon heat pipe and the cooling water. Fig. 6 shows the effect of the cooling methods on the performance of the cooling process of the activated carbon. In this experiment, the activated carbon was cooled down from 80–30°C. When using only the thermosiphon heat pipe or only cooling water, the cool-down times are approximately 5,640 and 2,400 s, respectively. When both the thermosiphon and cooling water are used, the cool down time is reduced to 1,800 s. The mass flow rate and temperature of the cooling water was kept constant at 0.03 kg/s and 27°C, respectively.

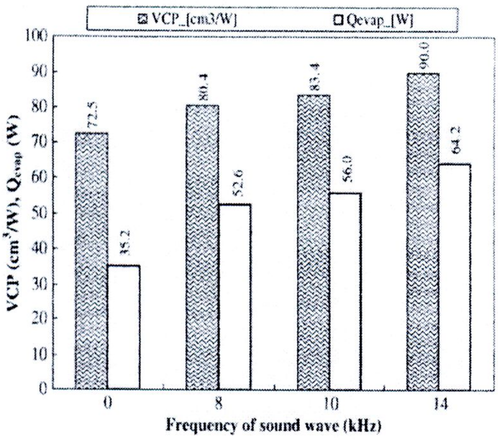

Fig. 8. The effect of the sound wave on the heat transfer rate and the VCP

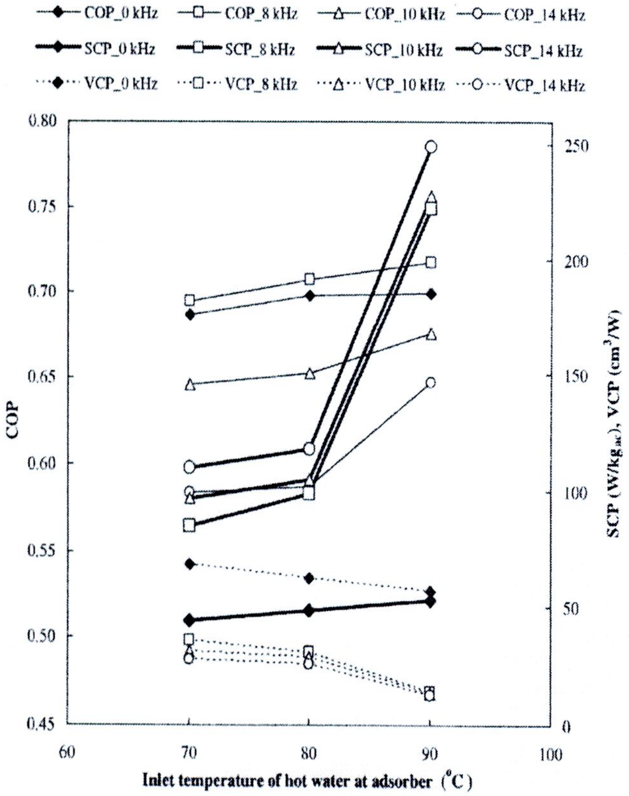

Fig. 9. Effect of the sound wave on system performance

Parameters Affecting Evaporator Performance

In the adsorption and evaporation phases, methanol got heat from the circulating water and vaporized in the evaporator. The inlet temperature and the mass flow rate of the circulating water were fixed at 30°C and 0.0018 kg/s, respectively. The performance of the evaporator was enhanced by the sound wave. Sonication generated alternating low- and high-pressure waves in the methanol liquid, leading to cavitation or the formation and collapse of small bubbles. Cavitational collapse produced intense local heating, high pressure, and enormous heating rates with very short lifetimes (Suslick 2008). Therefore, methanol was activated and vaporized easily. The energy of the sound wave could be adjusted by changing the wave frequency. In this experiment, the frequency of the sound wave was adjusted at 0 (or without wave), 8, 10, and 14 kHz.

The performances of the evaporator under the sound wave are shown in Figs. 7–9. The temperature profile of the adsorber in Fig. 7 showed that when using the sound wave, the temperature of the circulating water at an evaporator immediately changed compared with no wave (0 kHz).

Moreover, the minimum water temperature when using the sound wave was lower than the no-wave case by approximately 3°C. The result from Fig. 8 also agreed well with Fig. 7 because the heat transfer rate of the circulating water and the amount of vaporized methanol were increased with the frequency of the wave.

Table 2. Performance Comparison with Previous Works

	Present study	Tiansuwan et al. (1998)	Qu et al. (2001)	Wu et al. (2002)	Wang et al. (2006b)
Working pair	AC/Methanol	AC/Ethanol	AC/Methanol	AC/Methanol	AC/Methanol
Adsorber type	Double pipe	Double pipe	Plate finned shell and tube	Shell and tube	Shell and tube
Mass of activated carbon (g)	500	200	2,600 × 2	2,600 × 2	6,000 × 2
Inlet temperature of hot water at the adsorber (°C)	95	70–150 (hot oil)	95	100	100
Inlet temperature of cooling water at the condenser (°C)	5–15	25–45	30	6	25 (sea water)
Inlet temperature of water at the evaporator (°C)	28–30	20	5	21	30
Maximum COP	0.718	0.6	0.764	0.4	0.14
Maximum SCP (W/kg$_{ac}$)	248.90	—	—	150	35
Minimum VCP (cm^3/W)	12.22			2.00	6.67
Application	Air conditioning	Refrigeration	Air conditioning	Refrigeration	Ice making

Fig. 9 shows the performance of the adsorption system, COP, SCP, and VCP. When the sonic wave is applied to the end of evaporator, the COP [from Eq. (9)] should be calculated by

$$\mathrm{COP} = \frac{Q_{\mathrm{evap}}}{Q_{1-2} + Q_{2-3} + Q_{\mathrm{sonic}}} \tag{9}$$

where Q_{sonic} = power supplied to the sonic generator. In this study, the power is 6.41, 27.94, and 65.85 W for the frequencies of 8, 10, and 14 kHz, respectively.

From the experiment, 8 kHz was the suitable wave frequency that gave the highest COP.

SCP and VCP increased and decreased with the increasing of wave frequency because of the shortened cycle time and greater evaporation heat.

Performance Comparison With Previous Works

The comparison of the adsorption system performance with previous works is summarized in Table 2. The COP of the designed system is higher than those of Tiansuwan et al. (1998), Wu et al. (2002), and Wang et al. (2006b). These results may be attributable to the effect of the sound wave that enhanced the methanol vaporization phenomenon in the evaporator. However, the performance of the presented system is slightly below Qu et al. (2001), in which a plate finned shell and tube adsorber were used. The double pipe adsorber is easier to construct and the system is easily installed with an ultrasonic generator to enhance thermal performance. The technique could be conducted in many applications such as solar thermal processes and waste heat recovery.

Conclusion

The application of a sound wave to an adsorption cooling system with an activated carbon-methanol working pair was proposed in this paper. The influence of heat source temperature on the adsorber and heat sink temperature at the condenser during the desorption or condensation phase was interpreted. The adsorber was cooled down appropriately during a cooling phase by the combination of two methods, cooling water and a thermosiphon heat pipe. The sound wave adjusting frequency in the range of 8–14 kHz reduced the evaporation temperature and time at the evaporator so that the system performance indicated by COP, SCP, and VCP are improved. The system performance was closely comparable to systems from literatures. The highest COP and SCP obtained from this system was 0.718 and 248.90 W/kg, respectively.

Acknowledgments

The writers gratefully acknowledge the financial support provided by the Thailand Research Fund under Contract No. MRG4780154; the Commission on Higher Education, Ministry of Education, and the graduate school of Chiang Mai University, Thailand; and the facilities supported by the Thermal Technology Research Laboratory, Mae Moh Training Center, and the Electricity Generating Authority of Thailand.

Notation

The following symbols are used in this paper:

c_p = specific heat (J/kg K);
H_{des} = heat of desorption (J/kg);
L = latent heat of vaporization (J/kg);
m = mass (kg);
P = pressure (Pa);
Q = heat transfer (J);
R = ideal gas constant of methanol [J/(kg K)];
T = temperature (°C);
t = time (s);
V = volume (cm^3); and
x = concentration.

Subscripts

ac = activated carbon;
ads = adsorption/adsorber;
cond = condenser;
cw = cooling water;
evap = evaporator;
hw = hot water;
in = inlet;
max = maximum;
met = methanol;
min = minimum;
out = outlet;
s = saturated;
sonic = sonic wave; and
w = water.

References

Bathen, D. (2003). "Physical waves in adsorption technology: An overview." *Sep. Purif. Technol.*, 33(2), 163–177.

Breitbach, M., and Bathen, D. (2001). "Influence of ultrasound on adsorption processes." *Ultrason. Sonochem.*, 8(3), 277–283.

Breitbach, M., Bathen, D., and Schmidt-Traub, H. (2003). "Effect of ultrasound on adsorption and desorption processes." *Ind. Eng. Chem. Res.*, 42(22), 5635–5646.

Critoph, R. E. (1988). "Performance limitations of adsorption cycles for solar cooling." *Solar Energy*, 41(1), 21–31.

Hamdaoui, O., Naffrechoux, E., Tifouti, L., and Petrier, C. (2003). "Effect of ultrasound on adsorption–desorption of *p*-chlorophenol on granular activated carbon." *Ultrason. Sonochem.*, 10(2), 109–114.

Juang, R. S., Lin, S. H., and Cheng, C. H. (2006). "A liquid-phase adsorption and desorption of phenol onto activated carbons with ultrasound." *Ultrason. Sonochem.*, 13(3), 251–260.

Leong, K. C., and Liu, Y. (2004). "Numerical modeling of combined heat and mass transfer in the adsorbent bed of a zeolite/water cooling system." *Appl. Therm. Eng.*, 24(16), 2359–2374.

Li, Z., Li, X., Xi, H., and Hua, B. (2002). "Effects of ultrasound on adsorption equilibrium of phenol on polymeric adsorption resin." *Chem. Eng. J.*, 86(3), 375–379.

Lu, Y. Z., Wang, R. Z., Jianzhou, S., Xu, Y. X., and Wu, J. Y. (2004). "Practical experiments on an adsorption air conditioner powered by exhaust heat from a diesel locomotive." *Appl. Therm. Eng.*, 24(7), 1051–1059.

Maggio, G., Freni, A., and Restuccia, G. (2006). "A dynamic model of heat and mass transfer in a double-bed adsorption machine with internal heat recovery." *Int. J. Refrig.*, 29(4), 589–600.

Mason, T. J. (1991). *Practical sonochemistry: User's guide to applications in chemistry and chemical engineering*, Ellis Horwood, Chichester, UK.

Penn, R., Yeager, E., and Hovorka, F. (1959). "Effect of ultrasonic waves on concentration gradients." *J. Acoust. Soc. Am.*, 31(10), 1372–1376.

Qu, T. F., Wang, R. Z., and Wang, W. (2001). "Study on heat and mass recovery in adsorption refrigeration cycles." *Appl. Therm. Eng.*, 21(4), 439–452.

Rege, S. U., Yang, R. T., and Cain, C. A. (1998). "Desorption by ultrasound: Phenol on activated carbon and polymeric resin." *AIChE J.*, 44(7), 1519–1528.

Schueller, B. S., and Yang, R. T. (2001). "Ultrasound enhanced adsorption and desorption of phenol on activated carbon and polymeric resin." *Ind. Eng. Chem. Res.*, 40(22), 4912–4918.

Suslick, K. S. (2008). "Executive summary: The chemical and physical effects of ultrasound." (http://www.scs.uiuc.edu/suslick/execsummsono.html) (Dec. 23, 2008).

Tamainot-Telto, Z., and Critoph, R. E. (2003). "Advance solid sorption air conditioning modules using monolithic carbon-ammonia pair." *Appl. Therm. Eng.*, 23(6), 659–674.

Tiansuwan, J., Hirunlabh, J., and Kiatsiriroat, T. (1998). "Activated carbon-ethanol: An alternative working substance for adsorption cooling system." *J. Energy, Heat Mass Transfer*, 17(1), 65–73.

Wang, D. C., Xia, Z. Z., and Wu, J. Y. (2006a). "Design and performance prediction of a novel zeolite-water adsorption air conditioner." *Energy Convers. Manage.*, 47(5), 590–610.

Wang, D. C., and Zhang, J. P. (2009). "Design and performance prediction of an adsorption heat pump with multi-cooling tubes." *Energy Convers. Manage.*, 50(5), 1157–1162.

Wang, L. W., Wang, R. Z., Wu, J. Y., Xu, Y. X., and Wang, S. G. (2006b). "Design, simulation and performance of a waste heat driven adsorption ice maker for fishing boat." *Energy*, 31(2-3), 244–259.

Wang, R. Z., Wu, J. Y., Xu, Y. X., and Wang, W. (2001). "Performance research and improvements on heat regenerative adsorption refrigerator and heat pump." *Energy Convers. Manage.*, 42(2), 233–249.

Wu, J. Y., Wang, R. Z., and Xu, Y. X. (2002). "Experimental results on operating parameters influence for an adsorption refrigerator." *Int. J. Therm. Sci.*, 41(2), 137–145.

Yang, G. Z., et al. (2006). "Research on a compact adsorption room air conditioner." *Energy Convers. Manage.*, 47(15-16), 2167–2177.

Yaws, C. L. (1992). *Thermodynamic and physical property data*, Gulf Publishing, Houston.

Young, F. R. (1989). *Cavitation*, McGraw-Hill, New York.

Zhang, G., Wang, S., and Liu, Z. (2003). "Ultrasonic regeneration of granular activated carbon." *Environ. Eng. Sci.*, 20(1), 57–64.

Zhang, L. Z. (2000). "Design and testing of an automobile waste heat adsorption cooling system." *Appl. Therm. Eng.*, 20(1), 103–114.

International Publications

1.2 Performance analysis of a modular adsorption cooling system with sonic vibration in the adsorber. Journal of Experiment Heat Transfer, 10 May 2011, (Article inpress).

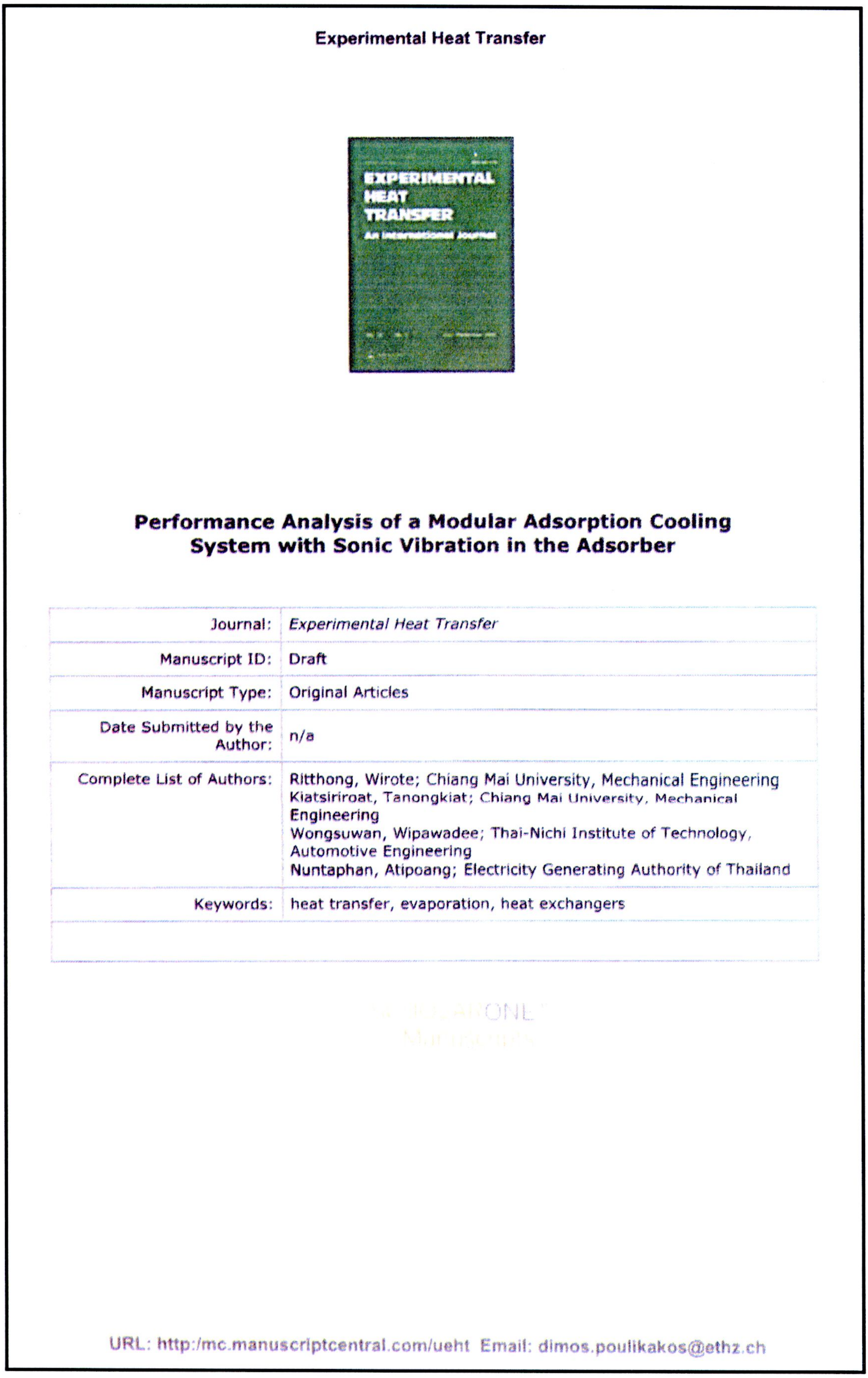

Experimental Heat Transfer

Performance Analysis of a Modular Adsorption Cooling System with Sonic Vibration in the Adsorber

Journal:	*Experimental Heat Transfer*
Manuscript ID:	Draft
Manuscript Type:	Original Articles
Date Submitted by the Author:	n/a
Complete List of Authors:	Ritthong, Wirote; Chiang Mai University, Mechanical Engineering Kiatsiriroat, Tanongkiat; Chiang Mai University, Mechanical Engineering Wongsuwan, Wipawadee; Thai-Nichi Institute of Technology, Automotive Engineering Nuntaphan, Atipoang; Electricity Generating Authority of Thailand
Keywords:	heat transfer, evaporation, heat exchangers

Performance Analysis of a Modular Adsorption Cooling System with Sonic Vibration in the Adsorber

Wirote Ritthong, Tanongkiat Kiatsiriroat
Department of Mechanical Engineering, Chiang Mai University,
Chiang Mai 50200, Thailand

Wipawadee Wongsuwan,
Department of Automotive Engineering, Thai-Nichi Institute of Technology,
Bangkok 10250, Thailand

Atipoang Nuntaphan
Thermal Technology Research Laboratory,
Coal Fired Power Plant and Mining Technological Skill Development Department,
Electricity Generating Authority of Thailand, Mae Moh, Lampang 52220, Thailand

ABSTRACT

This paper presents a performance evaluation of an adsorption cooling system using activated carbon-methanol as the working pair. The desorption process was enhanced by a sonic wave generator attached to the centre of the side of the adsorber. The results show that the sonic wave activation reduced the cycle time of the heating-condensation process and improved the system performance in terms of COP, SCP and VCP. The highest COP, SCP and VCP achieved for this system were 0.619, 229.15 W per kg of activated carbon, and 17.61 cm^3 of adsorber volume per W, respectively.

Keywords: Performance analysis, Adsorption cooling, Sonic wave, Thermosyphon heat pipe

CORRESPONDING AUTHOR
Prof. Tanongkiat Kiatsiriroat, D. Eng.
Department of Mechanical Engineering
Faculty of Engineering, Chiang Mai University
Chiang Mai, Thailand, 50200.
Tel. 6653- 944146, Fax. 6653-944145
Email: kiatsiriroat_t@yahoo.co.th

1. INTRODUCTION

Adsorption cooling systems have been utilised in various applications, e.g., in household or automobile (bus, locomotive, and car) air-conditioners, for refrigeration, and for ice storage. The adsorption air-conditioner developed by Zhang [1] for a bus exhibited a COP of about 0.38. The adsorption cooling system described by Wang et al. [2] used activated carbon-methanol as the working pair in an adsorption system in which the adsorber was a tube and plate heat exchanger; this system exhibited a COP of 0.40 and 3.8 kW of cooling capacity.

Lu et al. [3] tested a zeolite-water working pair in a locomotive air-conditioner powered by exhaust gas and achieved a cooling power of 3-5 kW with a COP of around 0.21. The cabin temperature was between 4 and 6°C lower than the ambient temperature. Yang et al. [4] designed a compact adsorption air-conditioning system with a 1-kW cooling capacity and achieved a COP of about 0.446.

In addition to experimental work and prototype demonstrations, a number of theoretical studies based on mathematical modelling and simulation have been reported, e.g., Tiansuwan et al. [5], Leong and Liu [6], Maggio et al. [7], Wang et al. [8], Kim et al. [9], Wang and Zhang [10] and Ritthong et al. [11].

An adsorber and an evaporator are the key components of an adsorption cooling system. Recently, Wongsuwan et al. [12] have shown that sonic waves can improve the performance of a modular adsorption cooling system using activated carbon-methanol as the working pair. A sonic wave generator was found to enhance the heat transfer required for the boiling of methanol during the adsorption and evaporation processes and to reduce the evaporation time. The COP and SCP were 0.718 and 248.90 W/kg, respectively. Oh et al. [13] applied an ultrasonic wave to a phase change material (PCM). A container was filled with paraffin wax, which was the PCM. An ultrasonic probe was attached to the bottom of the container, and an electric heater covered the outside surface of the container. When the wave was applied to the paraffin wax, the PCM vibrated, resulting in a melting time that was around 2.5 times less than that of the case without an ultrasonic wave. Kim et al. [14] studied the vibration caused by an ultrasonic wave in the case of pool boiling and natural convection heat transfer. A wire-type electric heater was submerged in a liquid pool, and a wave was then transferred into the liquid. It was found that the vibration caused by the ultrasonic wave could promote rapid boiling.

A sonic wave was expected to enhance adsorber performance. The increased desorption rate would result in a higher COP and SCP. A sonic wave generator was used to enhance methanol decomposition in the adsorber during the desorption process. This research focused on the application of a sonic wave during the regeneration process in the adsorber. Extensive experimental work was performed to analyse the influence of a sonic wave on the COP, SCP and VCP of a modular adsorption cooling unit at various frequencies and various adsorber inlet heat source and heat sink temperatures. A sonic wave was applied to the external surface of the adsorber to enhance expulsion of methanol from the activated carbon. The goal of this research was to improve knowledge of the application of sonic waves.

The performance of an adsorption cooling system is represented by the coefficient of performance (COP), the specific cooling power (SCP) and the volumetric cold production (VCP). These parameters can be evaluated using:

$$SCP = \frac{Q_{evap}}{m_{ac} \times t_{ads}}, \tag{1}$$

$$VCP = \frac{V_{ads} \times t_{ads}}{Q_{evap}}, \tag{2}$$

and

$$COP = \frac{Q_{evap}}{Q_{1-2} + Q_{2-3} + Q_{sonic}}, \tag{3}$$

where t_{ads} is the adsorption time, V_{ads} is the volume of the adsorber and Q_{sonic} is the power supplied to the sonic wave generator.

2. SONIC WAVE INCEPTION

The mechanical wave induced by a sonic wave generator creates variations in pressure or density. When the wave propagates through a medium, it is attenuated by absorption, by cavitation bubbles, by particles, and at interfaces (Breitbach et al. [15]). The high sound intensities produce either nonlinear phenomena or acoustic cavitation that exceeds the liquid tensile stress. During the rarefaction cycle of a sonic wave, a large negative pressure is applied to the liquid, and small gas bubbles form during the expansion cycle of the sound wave that grow to many times their initial size over one or more cycles (Juang et al. [16]). The bubbles are either stable for many cycles or transient, so that they grow to critical size and then violently collapse during the compression part of the wave. The energy that is released causes extreme thermodynamic conditions in the vicinity of the imploding bubbles, such as very high temperatures and pressures, and large shear forces occur in the surrounding liquid (Mason [17]). As the bubbles collapse, localised areas of high temperature lead to slight increases in system temperature, and localised areas of high pressure in the fluid create high-speed micro-jets with high-pressure shock waves (Hamdaoui et al. [18]). These waves and the associated microdisturbances of cavitation bubbles near the surface of a solid reduce the mass transfer boundary layer and thus effectively increase mass transfer (Penn et al. [19]).

3. EXPERIMENTAL SET-UP

The research was based on a number of experimental sets. Figure 1 shows a schematic sketch of the modular adsorption cooling unit. The cooling unit consisted of 3 main parts: an adsorber, a condenser and an evaporator. The adsorber was made of a copper tube 7.62 cm in diameter and 100 cm high. The adsorber was filled with 0.5 kg of activated carbon made from coconut shell, with a mesh size of 8×16. The external surface of the adsorber was covered with a water jacket, and the whole unit was well insulated.

During the desorption process, hot water at 95 °C was circulated inside the water jacket at a rate of 0.08 kg/s to regenerate methanol vapour in the adsorber. During the cooling phase, cold water was circulated in the water jacket. To enhance decomposition of the working fluid in the adsorber, a model SUNON-DP200A "sonic wave generator" was attached to the centre of the side of the adsorber. The frequency range of this wave generator is 8-14 kHz.

The condenser in the adsorption system consisted of a copper tube 7.62 cm in diameter and 23 cm in length, with a copper coil 149 cm in length and 10 mm in diameter inside. During the condensation process, water at ambient temperature (24-28 °C) was circulated inside the copper coil at 0.06 kg/s.

The evaporator in the adsorption system had the same dimensions as the condenser. During the evaporation of methanol, cold water at 10-20 °C was circulated inside the copper coil at a flow rate of 0.0018 kg/s.

Temperature measurements were taken with a set of K-type thermocouples with an accuracy of ± 0.1 °C and recorded by a model TSUS-TASK24C temperature data logger. The sensors were installed in the activated carbon and at the water inlets and outlets of the adsorber, the condenser and the evaporator. The evaporator temperature was measured at the evaporator chamber wall by a thermocouple. The pressure inside the adsorber and the evaporator was measured by two pressure gauges, with an accuracy of ± 0.1 kPa. The methanol level inside the evaporator was observed with a sight glass. The flow rate of water was calculated using the mass of circulating water during a specified period of time. The digital weighing apparatus has an accuracy of ± 1 g.

Table 1 contains a summary of the experimental conditions. During the desorption process, the maximum temperature of the activated carbon varied between 80°C and 90°C. During the heating-condensation process, a sonic wave was applied to the external surface of the adsorber to enhance methanol decomposition and release from the activated carbon.

4. RESULTS AND DISCUSSION

The operation of adsorptive cycles is analysed and discussed through four aspects of the cycles: the thermal behaviour of the adsorption system, the parameters affecting the adsorber, the valve opening effect, and the parameters affecting the evaporator.

4.1 Thermal behaviour of adsorption system

Figure 2 shows the temperature profiles from four adsorption cycles with or without a sonic wave: the activated carbon bed (T_{ads}), the methanol in the evaporator (T_{evap}), and the inlet and outlet temperatures of the circulating water in the evaporator ($T_{w,evap,in}$ and $T_{w,evap,out}$). A sonic wave was applied to the adsorber during the desorption–condensation process. During each cycle, the temperature of the activated carbon varied from 70 to 90 °C. The vapour pressure inside the adsorber dropped from approximately 256.35 kPa to 19.44 kPa.

The cycle time decreases with increasing wave frequency. For a wave frequency of 14 kHz, the cycle time is around 25% less than that of the case without a wave. The explanation for this result is as follows:

The sonic wave penetrated from the jacket surface through the water covering the activated carbon container. The penetrating wave could promote vibration between the outer surface of the activated carbon container and the fluid media. The vibration of the activated carbon container would thus enhance the heat transfer rate between the activated carbon and the adsorbed methanol. Consequently, a higher methanol desorption rate would be achieved.

4.2 Parameters affecting adsorber performance

The relevant parameters that affected the adsorption system performance were the regeneration temperature, the water temperature in the condenser, and the cooling rate of the adsorber after the desorption process. The regeneration or heat source temperature is the inlet temperature of the hot water circulated through the water jacket. The mass flow rate of the hot water was 0.08 kg/s, and its temperature varied from 80 to 90°C. The desorbed methanol vapour flowed downward to condense in a condenser. The mass flow rate and the temperature of the water in the condenser were 0.06 kg/s and 24°C.

The effect of a hot water inlet temperature of 90°C on the volume of evaporated methanol ($V_{met.}$), and the COP, SCP and VCP of the adsorber for sonic wave frequencies of 0 kHz (no wave), 8 kHz, 10 kHz and 14 kHz is shown in Figures 3-6. The volume of evaporated methanol ($V_{met.}$), the COP and the SCP increase with increasing hot water temperature and sonic wave frequency, whereas the VCP decreases. Unlike the other indicators, a lower VCP indicates better efficiency. For a heat source temperature of about 90°C, the $V_{met.}$, COP, SCP and VCP vary from 13.46 – 51.92 mL (85.74-285.74%), 0.3783 – 0.5929 (8.83-49.05%), 40.36 – 172.77 W/kg of activated carbon (218.21-328.07%), and 17.61-75.38 cm^3 of adsorber volume per W (218.19-328.05%), respectively.

The experimental results indicate that 14 kHz is the wave frequency resulting in the highest expelled volume of methanol from the activated carbon, the highest COP and SCP and the lowest value of VCP.

During the desorption process, the desorbed methanol vapour from the activated carbon flowed downward and condensed in the condenser. The cooling water flowed inside the internal copper tube to remove the heat of condensation. The flow rate and temperature of water were kept constant at 0.06 kg/s and 24 °C. The adsorber cooling began at temperatures of 80 and 90 °C. The amount of condensate was inversely proportional to the hot water temperature in the adsorber.

4.3 Effect of valve open temperature

During the desorption process, the desorbed methanol vapour from the activated carbon flowed downward to be condensed in the condenser. The cooling water flowed inside the internal copper tube to remove the heat of condensation. The flow rate and temperature were kept constant at 0.06 kg/s and 24°C. The temperature of the circulating water at the inlet of the adsorber for the "valve open" condition was either 60 or 70°C, whereas adsorber cooling was initiated at a temperature of 90°C.

The effect of the open valve hot water inlet temperature on the volume of evaporated methanol ($V_{met.}$) and on the COP, SCP and VCP of the adsorber for sonic wave frequencies of 0 kHz (no wave), 8 kHz, 10 kHz and 14 kHz is shown in Table 2. For cases where a wave is applied, the volume of evaporated methanol ($V_{met.}$), the COP and the SCP increase with both the increasing temperature of the hot water at the "valve open" condition and the sonic wave frequency, whereas the VCP decreases. At an open valve temperature of about 70 °C, the $V_{met.}$, COP, SCP and VCP vary from 13.46 – 53.85 mL (85.74-300.07%), 0.3783 – 0.6196 (14.37-38.95%), 40.36 – 229.15 W/kg of activated carbon (218.21-328.07%), and 17.61-75.38 cm^3 of adsorber volume per W (218.19-328.05%), respectively.

4.4 Parameters affecting evaporator performance

In this section, the performance of the evaporator is presented. The evaporator was first filled with liquid methanol. The methanol then adsorbed heat from the circulating water, which resulted in the vaporisation of methanol and a decrease in the circulating water temperature. The flow rate of the cooling water was kept constant at 0.0018 kg/s, and its temperature was varied from 10 to 15 to 20°C.

The resulting performance of the evaporator as the cooling water temperature changes is shown in Table 3. The volume of methanol evaporated from the evaporator (V_{met}) increases with the temperature of the cooling water; for temperatures of 10, 15 and 20 °C, the evaporated methanol volume was 4.50 mL, 7.69 mL and 13.46 mL, respectively.

The COP and SCP increase with the increase in cooling water temperature, but the VCP decreases. These results could be explained as follows.

When the temperature of the cooling water rises, the amount of methanol that is vaporised increases. It follows that the volume of evaporated methanol during the next evaporation process will also increase, which results in a higher transfer rate for the evaporation process and better system performance.

4.5 Performance comparison with previous work

A comparison of the adsorption system performance with previous work is summarised in Table 4. The *COP* of the designed system is higher than those of Tiansuwan et al [5], Wu et al. [20] and Wang et al. [8]. The improved performance is a result of the effect of the sonic wave, which improves desorption of methanol from the activated carbon bed.

However, the performance of this system is slightly lower than that of Qu et al. [21], which used a plate finned shell and tube adsorber. However, the double pipe adsorber is easier to construct, and the system can easily be installed with a sonic wave generator to enhance its thermal performance. This technique could be used in many applications, such as solar thermal processes, waste heat recovery and others.

5. CONCLUSION

In this study, we proposed and tested the application of a sonic wave generator to the adsorber in an adsorption cooling system using activated carbon-methanol as the working pair. Desorption was accomplished using two methods: circulating hot water through the water jacket and applying a sonic wave in the range of 8-14 kHz. The sonic wave was used to increase the temperature in the adsorber to improve system performance, as indicated by the COP, SCP and VCP. The highest COP, SCP and VCP obtained from this system were 0.619, 229.15 W per kg of activated carbon, and 17.61 cm^3 of adsorber volume per W, respectively.

ACKNOWLEDGEMENT

The authors gratefully acknowledge the financial support provided by the Commission on Higher Education, Ministry of Education, and Graduate School, Chiang Mai University. Thailand and the facilities supported by the Thermal Technology Research Laboratory, Chiang Mai University and Mae Moh Training Center, Electricity Generating Authority of Thailand.

REFERENCES

1. L.Z. Zhang, Design and testing of an automobile waste heat adsorption cooling system, Appl. Therm. Eng., vol. 20, no. 1, pp. 103-114, 2000.
2. R.Z. Wang, J.Y. Wu, Y.X. Xu and W. Wang, Performance research and improvements on heat regenerative adsorption refrigerator and heat pump, Energ. Convers. Manage., vol. 42, no. 2, pp. 233-249, 2001.
3. Y.Z. Lu, R.Z. Wang, S. Jianzhou, Y.X. Xu and J.Y. Wu, Practical experiments on an adsorption air conditioner powered by exhaust heat from a diesel locomotive, Appl. Therm. Eng., vol. 24, no. 7, pp. 1051-1059, 2004.

4. G.Z. Yang, Z.Z. Xia, R.Z. Wang, D. Keletigui, D.C. Wang, Z.H. Dong and X. Yang, Research on a compact adsorption room air conditioner, Energ. Convers. Manage., vol. 47, no. 15-16, pp. 2167-2177, 2006.
5. J. Tiansuwan, J. Hirunlabh, J. and T. Kiatsiriroat, Activated carbon-ethanol: an alternative working substance for adsorption cooling system, J. Ener. Heat Mass Tran., vol. 17, no. 1, pp. 65-73, 1998.
6. K.C. Leong and Y. Liu, Numerical modeling of combined heat and mass transfer in the adsorbent bed of a zeolite/water cooling system, Appl, Therm. Eng., vol. 24, no. 16, pp. 2359-2374, 2004.
7. G. Maggio, A. Freni, A. and G. Restuccia, A dynamic model of heat and mass transfer in a double-bed adsorption machine with internal heat recovery, Int. J. Refrig., vol. 29, no. 4, pp. 589-600, 2006.
8. L.W. Wang, R.Z. Wang, J.Y. Wu, Y.X. Xu and S.G. Wang, S.G., Design, simulation and performance of a waste heat driven adsorption ice maker for fishing boat, Energy, vol. 31, no. 2-3, pp. 244-259, 2006.
9. C.N. Kim, W. Xiaolin, S.L. Yee, B.S. Bidyut, C. Anutosh, K. Shigeru, A. Atsushi and K. Takao, Experimental study on performance improvement of a four-bed adsorption chiller by using heat and mass ecovery, Int. J. of Heat and Mass Trans., vol. 49, pp. 3343-3348, 2008.
10. D.C. Wang and J.P. Zhang, Design and performance prediction of an adsorption heat pump with multi-cooling tubes, Energ. Convers. Manage., vol. 50, no. 5, pp. 1157-1162, 2009.
11. W. Ritthong, P. Jansatidpaiboon, T. Aim-eiam, W. Wongsuwan, A. Nuntaphan and T. Kiatsiriroat, Performance Analysis of Thermosyphon Assisted Adsorption Cooling

System, The 3rd International Conference on "Sustainable Energy and Environment, May 18-23, Bangkok, Thailand, 2009.

12. W. Wongsuwan, W. Ritthong, T. Kiatsiriroat and A. Nuntaphan, Performance analysis of a modular adsorption cooling system having sonic vibration at evaporator, ASCE. J. Ener. Engr., vol. 137, no. 2, pp. 99-107, 2011.
13. Y.K. Oh, S.H. Park and Y.I. Cho, A Study of the Effect of Ultrasonic Vibrations on Phase-Change Heat Transfer, Int. J. of Heat and Mass Trans., vol. 45, pp. 4631-4641, 2002.
14. H.T. Kim, Y.G. Kim and H.K. Byung, Enhancement of Natural Convection and Pool Boiling Heat Transfer via Ultrasonic Vibration, Int. J. of Heat and Mass Trans., vol. 47, pp. 2831-2840, 2004.
15. M. Breitbach, D. Bathen and H. Schmidt-Traub, Effect of ultrasound on adsorption and desorption processes, Ind. Eng. Chem. Res., vol. 42, no. 22, pp. 5635–5646, 2003.
16. R. S. Juang, S. H. Lin and C.H. Cheng, A liquid-phase adsorption and desorption of phenol onto activated carbons with ultrasound, Ultrason. Sonochem., vol. 13, no. 3, pp. 251–260, 2006.
17. T. J. Mason, Practical Sonochemistry: User's guide to applications in chemistry and chemical engineering, Ellis Horwood, Chichester, UK., 1991.
18. O. Hamdaoui, E. Naffrechoux, L. Tifouti and C. Petrier, Effect of ultrasound on adsorption–desorption of p-chlorophenol on granular activated carbon, Ultrason. Sonochem., vol. 10, no. 2, pp. 109–114, 2003.
19. R. Penn, E. Yeager, F. Hovorka, Effect of ultrasonic waves on concentration gradients, J. Acoust. Soc. Am., vol. 31, no. 10, pp. 1372–1376, 1959.

20. J.Y. Wu, R.Z. Wang and Y.X. Xu, Experimental results on operating parameters influence for an adsorption refrigerator, Int. J. Therm. Sci., vol. 41, no. 2, pp. 137-145, 2002.

21. T.F. Qu, R.Z. Wang and W. Wang, Study on heat and mass recovery in adsorption refrigeration cycles, Appl. Therm. Eng., vol. 21, no. 4, pp. 439-452, 2001.

NOMENCLATURE

COP	coefficient of performance
SCP	specific cooling power (W/kg)
VCP	volumetric capacity power (cm^3/W)
t	time (s)
T	temperature (°C)
V	volume (cm^3)

Subscripts

ac	activated carbon
ads	adsorption/ adsorber
cond	condenser
cw	cooling water
evap	evaporator
hw	hot water
in	inlet
met	methanol
out	outlet
sonic	sonic wave
w	water

Table 1. Summary of the testing conditions in this study.

Parameter	Value
Mass of activated carbon (mesh size 8 x 16)	0.5 kg
Volume of methanol	900 cm^3
Desorption process	
Inlet temperature of hot water	95 °C
Mass flow rate of hot water	0.08 kg/s
Maximum temperature of activated carbon	80, 90 °C
Frequency of sonic wave	0, 8, 10, 14 kHz
Condensation process	
Inlet temperature of water	24-26 °C
Mass flow rate of water	0.06 kg/s
Evaporation process	
Inlet temperature of cooling water	10, 15, 20 °C
Mass flow rate of cooling water	0.0018 kg/s
Adsorption process	
Inlet temperature of water	24- 26 °C
Mass flow rate of cooling water	0.035-0.045 kg/s

Table 2. Effect of valve open temperature.

	Tac_valve (°C)	Frequency of Sonic Wave (kHz)			
		0	8	10	14
V_{met} (mL)	60	8.54	13.46	23.08	50.92
	70	13.46	25.00	38.46	53.85
COP (-)	60	0.3304	0.3802	0.4975	0.5929
	70	0.3783	0.4418	0.5287	0.6196
SCP (W/kg_ac)	60	48.68	51.28	97.84	172.77
	70	40.36	128.43	155.22	229.15
VCP (m^3/W)	60	62.48	59.32	31.09	13.27
	70	75.38	23.68	19.6	17.61

Table 3. Parameters affecting evaporator performance.

	T_{cw_evap} (^{o}C)	Frequency of Sonic Wave (kHz)			
		0	8	10	14
V_{met} (mL)	10	4.50	5.77	6.75	7.20
	15	7.69	10.17	15.38	19.23
	20	13.46	25.00	38.46	51.92
COP (-)	10	0.1501	0.1553	0.1751	0.2019
	15	0.2600	0.3290	0.3992	0.4151
	20	0.3783	0.4418	0.5287	0.6196
SCP (W/kg_ac)	10	16.88	18.47	27.09	29.04
	15	36.61	51.53	55.10	68.50
	20	40.36	128.43	155.22	172.77
VCP (m^3/W)	10	180.23	164.69	112.29	104.73
	15	83.08	59.03	55.20	44.41
	20	75.38	23.69	19.60	17.61

Table 4. Performance comparison with previous works.

	Present study	Tiansuwan et al. [5]	Qu et al. [2]	Wu et al. [20]	Wang et al. [8]
Working pair	AC/Methanol	AC/Ethanol	AC/Methanol	AC/Methanol	AC/Methanol
Adsorber type	Double pipe	Double pipe	Plate finned shell and tube	Shell and tube	Shell and tube
Mass of activated carbon (grams)	500	200	2,600 x 2	2,600 x 2	6,000 x 2
Inlet temperature of hot water at adsorber (°C)	95	70-150 (hot oil)	95	100	100
Inlet temperature of water at condenser (°C)	24-26	25-45	30	6	25 (sea water)
Inlet temperature of cooling water at evaporator (°C)	10-20	20	5	21	30
Maximum COP	0.619	0.6	0.764	0.4	0.14
Maximum SCP (W/kg$_{ac}$)	229.15	-	-	150	35
Minimum VCP (cm^3/W)	17.61	-	-	2.00	6.67
Application	Refrigeration	Refrigeration	Air conditioning	Refrigeration	Ice making

LIST OF FIGURE CAPTIONS

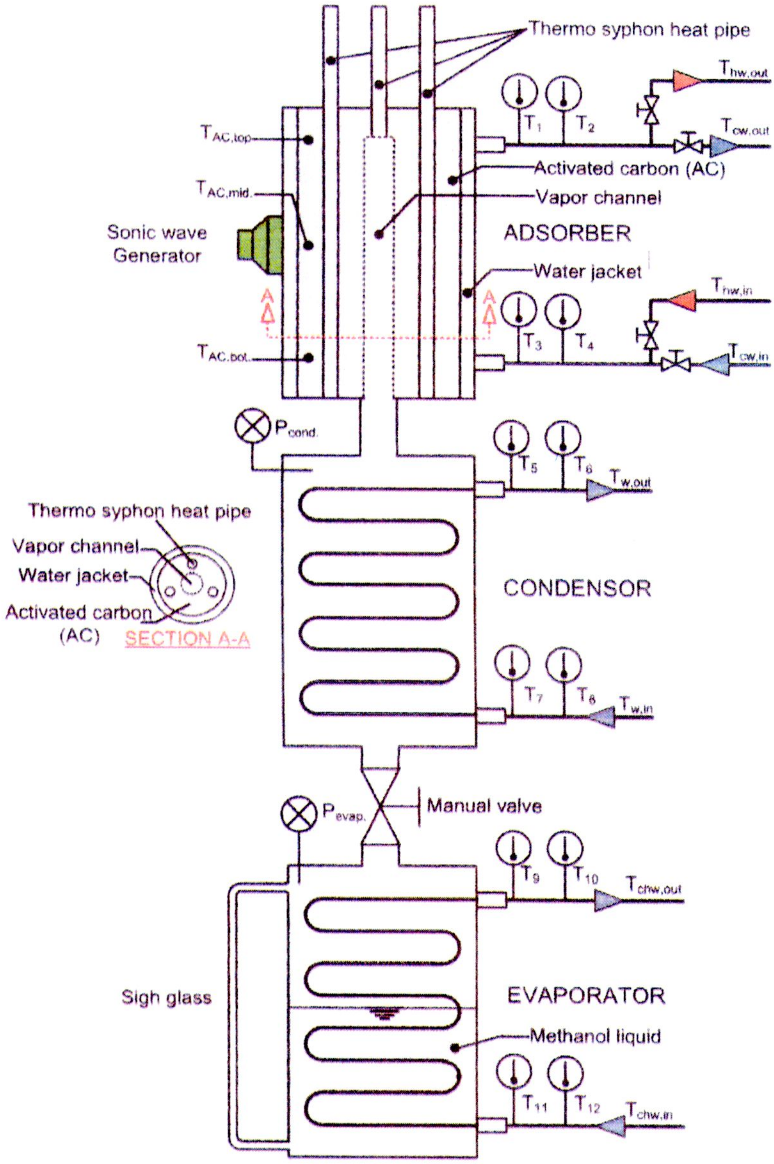

Figure 1. The modular solid adsorption cooling unit.

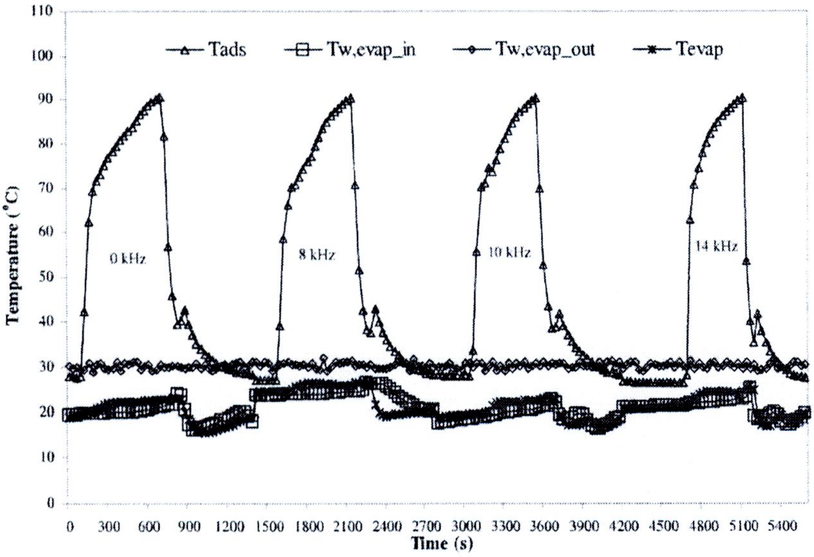

Figure 2. Temperature profiles of the adsorption system.

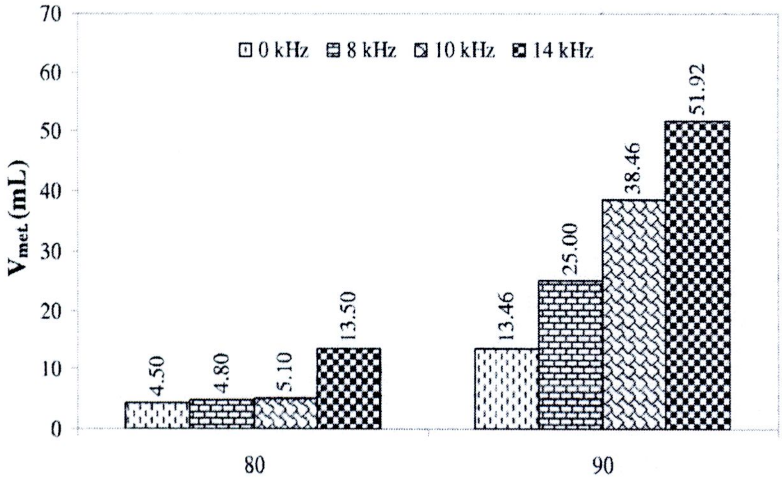

Figure 3. Effect of the hot water temperature at the inlet of the adsorber on the volume of methanol condensate.

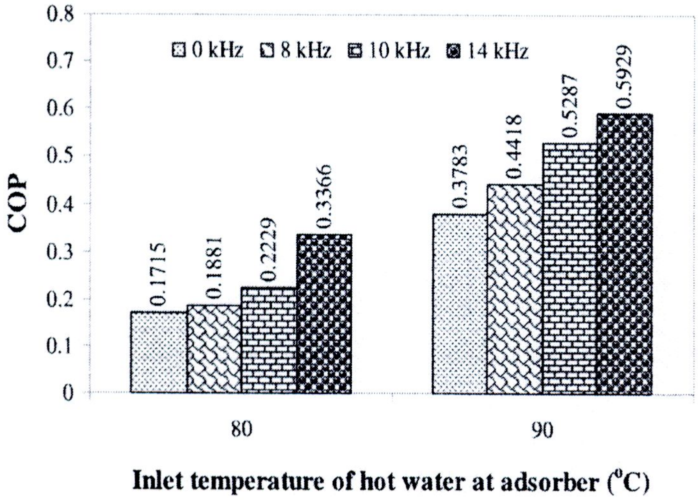

Figure 4. Effect of the hot water temperature at the inlet of the adsorber on system performance.

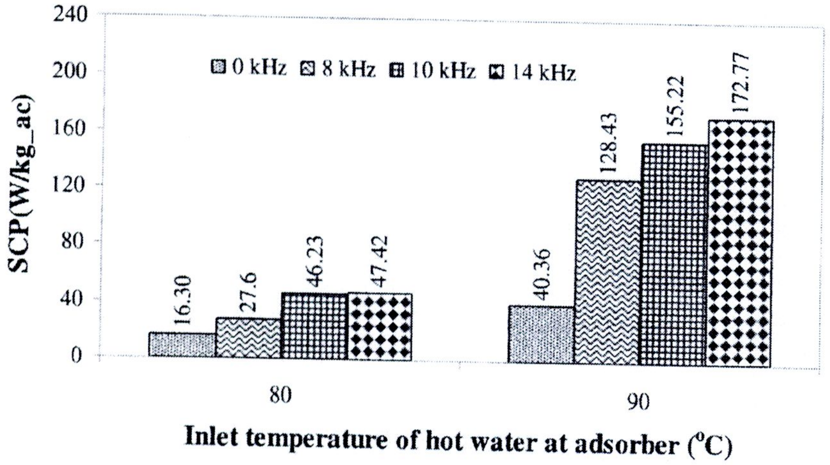

Figure 5. Effect of the hot water temperature in the adsorber on specific cooling power.

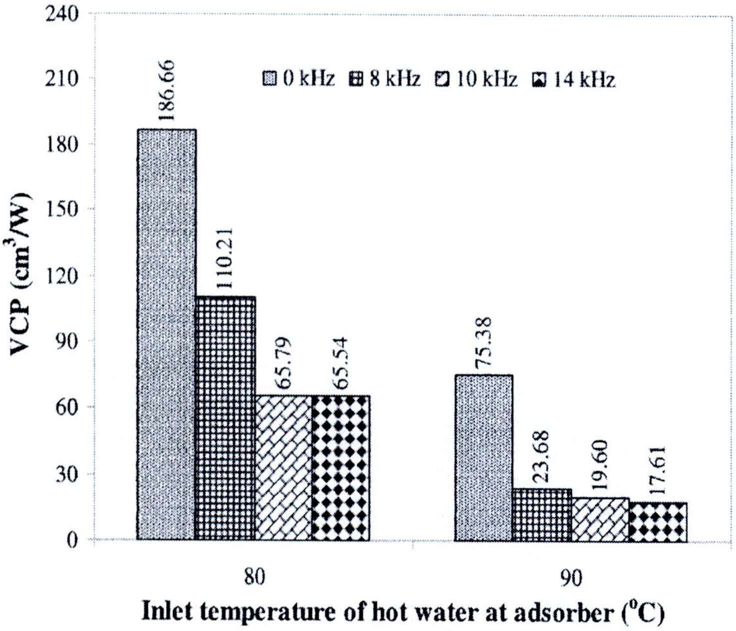

Figure 6. Effect of the hot water temperature at the inlet of the adsorber on volumetric cold production.

International Publications

1.3 Performance Analysis of Thermosyphon Assisted Adsorption Cooling System. World Renewable Energy Congress 2009-ASIA. The 3rd International Conference on "Sustainable Energy and Environment (SEE 2009)", 18-23 May 2009, Bangkok, Thailand.

Second Announcement & Call for Papers

WREC 2009 - Asia

www.wrec2009asia.com

World Renewable Energy Congress 2009 - Asia

19-22 May, 2009
BITEC, Bangkok, Thailand

Important Dates

30 January 2009	**Abstract submission**
15 February 2009	Notification of acceptance
15 April 2009	Deadline for full paper submission
15 April 2009	Deadline for registration

Incorporating

RENEWABLE ENERGY ASIA 2009
ASIA INTERNATIONAL RENEWABLE ENERGY CONFERENCE AND EXHIBITION

SEE 2009
The 3rd International Conference on Sustainable Energy & Environment (SEE 2009)

SEE Forum
The 5th SEE Forum Meeting

Co-organised by

JGSEE
The Joint Graduate School of Energy and Environment

CMP
United Business Media

In Collaboration with

Kyoto University

Secretariat of WREC 2009 - Asia
The Joint Graduate School of Energy and Environment (JGSEE)
King Mongkut's University of Technology Thonburi
126 Pracha-Uthit Road, Bangmod, Tungkru, Bangkok 10140 Thailand
Tel: +662 4708309-10 Ext. 4133, 4134, 4152, Fax: 662 8729805
E-mail: secretariat@wrec2009asia.com

Under Patronage of WREN

Officially Supported by

THAILAND
convention & exhibition bureau

Performance Analysis of Thermosyphon Assisted Adsorption Cooling System

Wirote Ritthong[1,2], Phatsawan Jansatidpaiboon[1], Teeranon Aim-eiam[1],
Wipawadee Wongsuwan[1,*], Atipoang Nuntaphan[3], and Tanongkiat Kiatsiriroat[1]

[1]Department of Mechanical Engineering, Chiang Mai University (CMU), Chiang Mai, Thailand, 50200
[2]Mechanical Engineering Department, Faculty of Engineering, Rajamangala University of Technology Phra Nakorn, Bangkok, 10800
[3]Thermal Technology Research Laboratory, Mae Moh Training Center, Electricity Generating Authority of Thailand (EGAT), Mae Moh, Lampang, Thailand, 52220
[*]Corresponding Author: wipawadee.w@gmail.com, vibhavadee@yahoo.com

Abstract: *Our research paper analyzes the use of thermosyphon to enhance heat transfer of the adsorption cooling system. The experimental adsorption system in vertical alignment has three components: an adsorber, a condenser and an evaporator, using activated carbon (AC) /methanol as the working pair. The adsorber was cooled during adsorption phase by various approaches; (i) cooling water, (ii) thermosyphon heat pipes either with or without fins, (iii) cooling water and thermosyphon, and (iv) cooling water and closed-loop oscillating heat pipe (CLOHP). The test conditions are varied by; adsorber temperature during desorption phase (70 °C, 80 °C, 90 °C), and cooling water temperature supplied to the condenser (5 °C, 10 °C, 15 °C). It was found that thermosyphon and CLOHP could efficiently enhance heat transfer of the adsorber, and then reduced cool down time during adsorption phase. The coefficient of performance (COP) and specific cooling power (SCP) increased with desorption temperature, but decreased with cooling water temperature at the condensor, which were contrary to volumetric cold production (VCP). The tested COP and SCP were equivalent to those reported in literatures. Additionally, the use of self-control valve, to facilitate methanol vapor transfer between adsorber and evaporator/condenser, was not reduced the system performance. Therefore, this adsorption system could work automatically, when reducing a number of valves normally required for the adsorption cooling system.*

Keywords: Adsorption Cooling, Control Valve, Experiment, Thermosyphon, Heat Transfer Enhancement

1. INTRODUCTION

The adsorption cooling system is environmental-friendly and considerably attractive alternative to the traditional vapor compression cooling system based on CFC refrigerants. Adsorption cooling normally employed non-polluting refrigerants, e.g., activated carbon (AC)-methanol, AC-ethanol, silica gel-water, zeolite-water, zeolite-ammonia, etc. The advantages of the adsorption cooling system are that (i) low maintenance required due to no major moving parts (ii) environmental-friendly adsorbent–adsorbate pair and (iii) potential to recover of waste heat which consequently minimizing thermal pollution [1]. Unfortunately, the application of adsorption cooling system is not easily widespread that it has been limited by its rather long cycle time and low coefficient of performance (COP) and specific cooling power (SCP). To increase an opportunity in competing with the conventional system, it is necessary to enhance heat and mass transfer either within or among system components, as well to reduce cycle time and equipment size. Therefore, our work investigated the use of internal heat pipes, either thermosyphon or closed-loop oscillating heat pipe (CLOHP), to enhance heat removal during adsorption period. In the other point of view, the adsorption system was generally controlled by a lot of valves. Therefore, our research also discussed the effect of a self-control valve that can reduce number of valves.

2. METHODOLOGY

The research methodology composed of design and fabrication of adsorber, assembly major components together, installation the system to the heat source and sink systems, testing and analysis of single-effect adsorption cooling system. The test unit in Fig. 1 was set up in vertical alignment to reduce volume and space required.

2.1 Experimental Set up

The schematic sketch of the single-effect of vertical solid adsorption refrigeration unit is shown in Fig. 1. It consists of 3 main parts, an absorber, a condenser and an evaporator. The working pair is activated carbon (AC) and methanol. The heat source and heat sink for adsorber, evaporator and condensor is emulated by the heating/cooling water circulated from the two water reservoirs. The electric heater and refrigeration system inside these reservoirs maintained stability of the inlet heating and cooling water. The specification of all major components and experimental conditions are summarized in Table 1. The influence of two variables were tested; (i) maximum temperature of the adsorber during desorption phase corresponding with the hot water temperature supplied to the adsorber (70 °C, 80 °C, 90 °C), and (ii) cooling water temperature supplied to condenser that similar to condensation temperature (5 °C, 10 °C, 15 °C). The adsorption cycle contains two main phases; desorption and adsorption. During adsorption phase, the heat transfer (water) media flows into an evaporator and the methanol vaporizes. The vapor of methanol flows upward and adsorbs to the activated carbon bed, resulting in increasing of activated carbon temperature. Cold is produced at the evaporator while cooling is required at the adsorber. In the other phase, heat is supplied to the adsorber to regenerate the refrigerant from the adsorber that flows down to the condensor, where condensation takes place.

The first part of our work focused on the cooling process of the cylindrical adsorber, which two major approaches were applied; (i) cooling water circulated through the external water jacket of the adsorber, and (ii) internal heat pipes inserted into the (activated carbon) adsorbent bed, which their combinations lead to 6 cooling methods. A thermosyphon heat pipe, one type of heat exchanger, has been used in many industrial processes because of its high advantages such as high thermal conductivity, low cost and easy to be constructed [2-3]. The adsorber was cooled based on the following 6 cooling cases during adsorption phase (including isosteric cooling period and isobaric cooling and adsorption period);

Case (1): Cooling water circulating through the external water jacket of the adsorber.

Case (2): Thermosyphon heat pipes *with* fins. Four heat pipes having smooth and circular fins were installed inside the adsorber to enhance heat release. Each thermosyphon is filled with (methanol) working fluid with 25% volume ratio to its evaporator sections.

Case (3): Thermosyphon heat pipes *without* fins. Three heat pipes having (methanol) working fluid filled with 50% volume ratio were installed into the adsorbent bed.

Case (4): Closed-loop oscillating heat pipe (CLOHP). The CLOHP, having 2-mm of copper tube diameter, with 30 up-and-down turns, and 1500-mm height, is used for cooling the adsorber (Fig.2). A pressure gauge is installed into the adsorber to measure the adsorber pressure.

Case (5): Cooling water and Thermosyphon with fins that is the combination of case (1) and (2)

Case (6): Cooling water and Thermosyphon withou fins that is the combination of case (1) and (3)

Case (7): Cooling water and CLOHP, the integration of case (1) and (4)

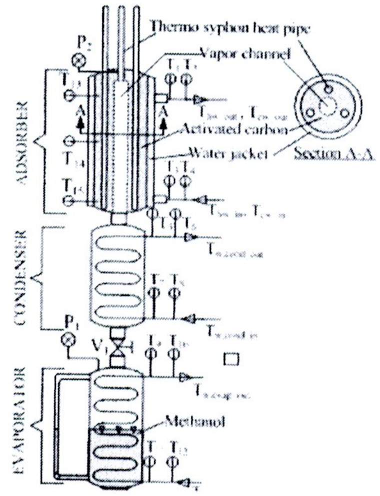

Fig. 1 Schematic sketch of the experiment apparatus

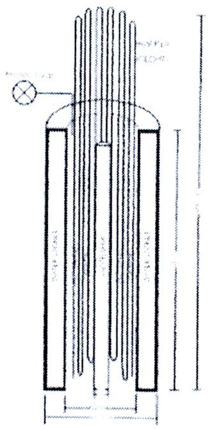

Fig. 2 Closed-loop oscillating heat pipe in adsorber

Temperature measurement was recorded at various locations in the system by the K-type thermocouples having ± 0.1 °C accuracy and a data logger from TASK. The sensors were installed into activated carbon bed, the inlet and the outlet of heating/cooling water at water jacket of the adsorber, and internal water coils of the condenser and the evaporator. The pressures inside the adsorber and the evaporator were measured by two pressure gages having ± 0.1kPa accuracy. The cycle mass of refrigerant was measured by the side-glass tube (see also Fig.1).

The heat source or driven temperature is defined by the temperature of the hot water as heat exchange fluid. In this analysis, maximum temperature of AC during desorption process was varied by 3 values; 70, 80 and 90 °C. The variations of COP and SCP with desorption temperature were investigated. If was found from literature review [4] based on numerical simulation that both COP and SCP would increase with the driven temperature of heat exchange fluid. The increase of the hot fluid temperature will in turn lead to an increase in the desorption temperature. The cycle mass of refrigerant will also increase with an increase in the desorption temperature [4]. Therefore, the cooling energy will also increase. Since the cycle time does not increase very much with the increase of hot water temperature, the SCP value also increases. A high heat source temperature not only improves the system performance, but also requires safety issues and heat loss reduction due to high temperature heat exchange fluid in actual applications. All experiments on our cooling process of the adsorber used the similar shape, geometry and dimensions of the adsorber as well as cooling water jacket; the differences are only the design of the thermosyphon or CLOHP. The case (5), (6) and (7) were repeated for the varying desorption temperatue and condensation temperature. In the case of using control valve, additional variable was the set point temperature to open/close the control valve (see also Table 1).

Table 1 Specification of experimental unit and the test conditions.

Parameter	Value	Unit
Specification		
1. Adsorber		
- Adsorber diameter	762	mm
- Adsorber height	1000	mm
- Mass of activated carbon (mesh size 8 x 16)	500	g
- case (2) Thermosyphon diameter/height/qty. heat pipe	10/1500/4	mm/mm/pipes
- with smooth and spiral circular fins		
- heat pipe working fluid (methanol) volume	18 mL or 25%	mL or % filling per pipe
- case (3) Thermosyphon diameter/height/no of heat pipe	10/1500/3	mm/mm/pipes
- filling volume of methanol in evaporator section	50%	% filling per pipe
- case (4) CLOHP diameter/height/qty. of turns	2/1500/30	mm/mm/turns
2. Evaporator		
- Evaporator diameter	762	mm
- Evaporator height	250	mm
- Volume of methanol	900	cm^3
- Diameter of internal coil of heat transfer fluid (water)	12.7	mm
3. Condensor		
- Condensor diameter	762	mm
- Condensor height	230	mm
- Diameter of internal coil of heat transfer fluid (water)	12.7	mm
Experimental Conditions		
1. Desorption process		
Inlet temperature of hot water	80 – 95	°C
Mass flow rate of hot water	0.08	kg/s
**Maximum (desorption) temperature of activated carbon*	*70, 80, 90*	℃
**Set point temperature of control valve*	*60, 70, 80*	℃
Initial adsorber state:		
- heating process: temperature/pressure	27/12	°C/kPa
- heating and desorption: tempertaure/pressure	(70,80,90)/40	°C/kPa
2. Condensation process		
**Inlet temperature of cooling water*	*5, 10, 15*	℃
Mass flow rate of cooling water	0.06	kg/s
3. Evaporation process		
Inlet temperature of water	28 – 35	°C
Mass flow rate of cooling water	0.0018	kg/s
4. Adsorption process		
Inlet temperature of water	28 – 35	°C
Mass flow rate of cooling water (case (1),(5),(6),(7))	0.05	kg/s

* *Itallic means variables in these experiments.*

2.2 Adsorber with CLOHP

The schematic and photo of our test unit having CLOHP inserted into the adsorbent bed is shown in Fig.3, and the cross section of adsorber is illustrated in Fig.2. The condenser and evaporator design is similar to those used in case (1) to (3).

2.3 On-off self-control valve

The self-control valve has potential to control adsorption and desorption processes. This section considers the influence of a temperature-control valve to control flow direction of working fluid. The temperature set point is determined by the appropriated saturated pressure of the adsorber during desorption phase. The experimental setup is shown in Fig. 4. Two valves were placed into two lines between adsorber-evaporator and adsorber-condenser. The activated carbon (AC) bed was packed inside the adsorber that made of copper tube. Four heat pipes with fin were installed into the adsorber bed. The experiments were carried out either using manual valve or control valve. The methanol vapor was flown among three components that its direction was controlled by valves. The methanol vapor was moved by pressure difference between up- and down-stream components. The on-off control valve was set up by two pressure levels, (i) high pressure in the condenser and (ii) low pressure in evaporator. To ease the control algorithm, the measured saturated temperature in corresponding with saturated pressure of adsorber is translated into the signal to control valve opening. When the adsorber temperature reaches the set point temperature, the valve is automatically fully opened, until desorption and consensation process is completed. Then the control valve is automatically closed.

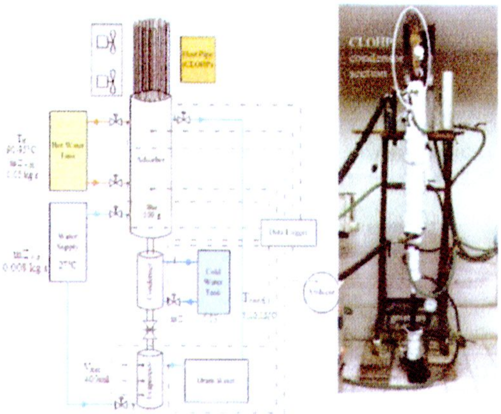

Fig. 3 Experimental set up for the CLOHP test

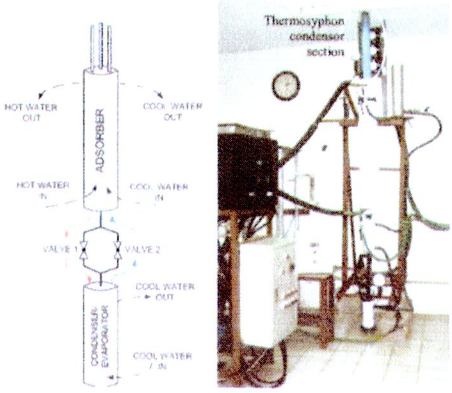

Fig. 4 Experimental set up of the control valve test

3. RESULTS AND DISCUSSION

3.1 System performance indicators

The performance of adsorption cooling system could be determined by achieved cooling rate at the evaporator, cycle time (including 4 periods; isosteric heating, isobaric heating or desorption, isosteric cooling, and isobaric cooling or adsorption), and lowest evaporator temperature (T_{ev}). Three performance indicators are normally computed to compare various design concepts; i.e., the coefficients of performance (COP), the specific cooling power (SCP) and the volumetric cold production (VCP). These parameters could be evaluated from

$$COP = \frac{Q_{useful}}{Q_{input}} = \frac{Q_{evap}}{Q_{1-2} + Q_{2-3}}, \tag{1}$$

$$SCP = \frac{Q_{evap}}{m_{ac} \times t_{ads}}, \tag{2}$$

$$VCP = \frac{V_{adsorber} \times t_{ads}}{Q_{evap}}. \tag{3}$$

where t_{ads} is the adsorption time and $V_{adsorber}$ is the volume of adsorber. The energy input to the adsorber during desorption process are; Q_{1-2} (isosteric heating process 1-2) resulting in the increasing of temperature from T_1 to T_2, Q_{2-3} (isobaric heating process 2-3) resulting in the increasing of temperature from T_2 to T_3.

$$Q_{1-2} = m_{ac}\left(c_{p,ac} + c_{p,met}x_{\max}\right)(T_2 - T_1), \tag{4}$$

$$Q_{2-3} = m_{ac}\left\{\left[c_{p,ac} + c_{p,met}\frac{(x_{\max} + x_{\min})}{2}\right](T_3 - T_2) + (x_{\max} - x_{\min})H_{des}\right\}, \tag{5}$$

$$H_{des} = \left(R \ln\left(\frac{P_2}{P_1}\right)\right) / \left(\frac{1}{T_1} - \frac{1}{T_2}\right). \tag{6}$$

where m_{ac} is the mass of activated carbon in the adsorber, $x_{\max}$ and $x_{\min}$ are the maximum and minimum concentration of methanol in activated carbon, $c_{p,ac}$ and $c_{p,met}$ are the specific heats of activated carbon and methanol. H_{des} is the average heat of desorption/adsorption evaluated by using the Clausius-Clapeyron equation [5], and R is the ideal gas constant, P_1 and P_2 are the saturated vapor pressures at the beginning and the end states of isosteric heating, respectively.

3.2 Effect of cooling method during cooling and adsorption periods

The cylindrical adsorber is cooled by either circulation of cooling water or heat pipes (thermosyphon or CLOHP), or their combinations. The main target is to reduce cooling time that will further reduce overall cycle time, and to enhance better system performance. Fig. 5 compares adsorber temperature profile during cooling and adsorption period, cooling time, and cooling rate, based on different cooling methods. The cooling capacities are also summarized in Table 2. The activated carbon is cooled down from 80 °C to 30 °C. It is found that the cool down time is the shortest in case of using cooling water combined with CLOHP; while single CLOHP gave the longest cool down time. When using only thermosyphon heat pipe or only cooling water, the cool down times are approximately 5,640 s and 2,400 s, respectively. When both of thermosyphon and cooling water is used, the cool down time is reduced to 1,800 and 1,860 s, respectively. The thermosyphon either with- or without- fins gave insignificant differences of cooling capacities. Although three thermosyphons in case (3) had no fins, they could provide better cooling rate. The reason is because of their larger filling volume ratio of the methanol (50%) as compared to the case of four thermosyphons with fins (case (2)). The maximum cooling rate about 13.77 W was achieved when both cooling water and CLOHP were applied, which the cooling time could be reduced by 37.5% in comparison with the case of using cooling water only.

3.3 Influence of on-off self-control valve

The experimental experiences suggested that the suitable setting temperature for on-off control valve is the temperature difference (lower) than maximum adsorber temperature about 10-15 °C. The appropriated temperatures were; maximum adsorber temperature about 85 °C and the setting temperature for self-control valve opening at 70 °C. The effect of control valve on the system performance could be observed from Table 3.

3.4 Comparison of adsorption cooling system performance

The performance of the adsorption cooling system is not only influenced by cooling approaches, but also their operating conditions, i.e., desorption temperature (T_{des}) and cooling water temperature at the condensor (T_{cd}). Depending on our findings that are discussed in section 3.2, the combination between two cooling approaches, cooling water and thermosyphon/CLOHP resulted in better cooling capacities, then the comparison on the system performance in this section would be focused on case (5) to (7). The adsorption cooling system performances, computed for various adsorber cooling methods, operating conditions, and case using control valve, are presented in Table 3. The COP increased with the increasing desorption temperature, except the case of integrated cooling water and thermosyphon with fins, and the case of control valve. However, SCP increased drastically with the increasing T_{des}, but reduced with the increasing T_{cd}. In contrary, VCP that lower value is better, could be reduced with the increasing T_{des}, but increased due to the drawback of higher T_{cd}. The use of control valve did not reduce the system performance. The resulted COP and SCP are comparable to the range found in the literatures. However, our VCP so far needed to be reduced.

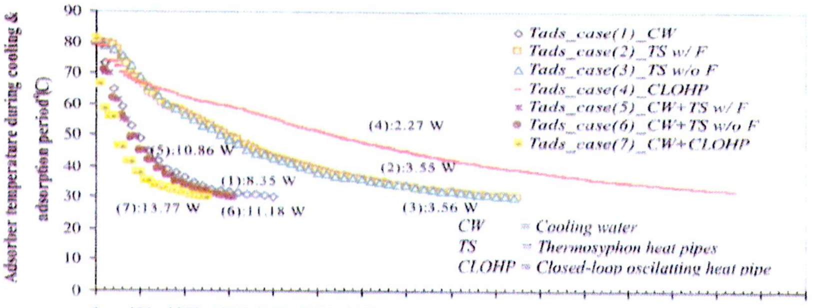

Fig. 5 Comparison of adsorber temperature profile, cooling time and cooling rate (in cooling and adsorption period)

Table 2 Cooling capacities of the adsorber during cooling and adsorption period

Case	**Cool down time (sec)**	**Cool down time (min)**	$(\Delta T)/t$ (°C/sec)	**Heat removal amount (kJ)**	**Cooling rate (W)**
(1)	2400	40	0.0208	20.04	8.35
(2)	5700	95	0.0088	20.25	3.55
(3)	5640	94	0.0088	20.08	3.56
(4)	8640	144	0.0056	19.64	2.27
(5)	1860	31	0.0270	20.21	10.86
(6)	1800	30	0.0278	20.13	11.18
(7)	1500	25	0.0341	20.65	13.77

Table 3 Comparison of adsorption cooling system performance

Case	Adsorber design/ Cooling method Desorption/Condensation temperature	Lowest T_{ev} (°C)	Cooling power (W)	COP (-)	SCP (W/kg)	VCP (cm^3/W)
1. Case (5)	***Cooling water + Thermosyphons without fins***					
	- (T_{des} (°C),T_{cd} (°C)) = (70,10)	18.5	22.21	0.69	44.42	68.48
	- (T_{des} (°C),T_{cd} (°C)) = (80,10)	16.9	35.21	0.70	70.42	43.20
	- (T_{des} (°C),T_{cd} (°C)) = (90,10)	18.1	41.51	0.70	82.40	36.90
	- (T_{des} (°C),T_{cd} (°C)) = (80,5)	16.5	42.34	0.70	84.68	35.92
	- (T_{des} (°C),T_{cd} (°C)) = (80,15)	18.6	38.79	0.69	77.57	39.22
2. Case (6)	***Cooilng water + Thermosyphons with fins + Manual valve***					
	- (T_{des} (°C),T_{cd} (°C)) = (70,10)	20.1	33.78	0.40	67.55	45.03
	- (T_{des} (°C),T_{cd} (°C)) = (80,10)	17.3	41.85	0.38	83.69	36.35
	- (T_{des} (°C),T_{cd} (°C)) = (90,10)	16.8	62.80	0.26	125.60	24.22
	- (T_{des} (°C),T_{cd} (°C)) = (80,5)	18.0	49.62	0.39	99.23	30.66
	- (T_{des} (°C),T_{cd} (°C)) = (80,15)	19.8	38.87	0.32	77.73	39.13
3. Case (7)	***Cooling water + CLOHP***					
	- (T_{des} (°C),T_{cd} (°C)) = (70,10)	22.4	45.70	0.30	91.40	33.28
	- (T_{des} (°C),T_{cd} (°C)) = (80,10)	19.7	46.80	0.37	93.60	32.50
	- (T_{des} (°C),T_{cd} (°C)) = (90,10)	16.0	55.70	0.33	111.40	27.31
	- (T_{des} (°C),T_{cd} (°C)) = (80,5)	19.4	51.50	0.45	103.00	29.53
	- (T_{des} (°C),T_{cd} (°C)) = (80,15)	20.6	45.90	0.33	91.80	33.14
4. Case(6) and control valve	***Cooling water + Thermosyphon with fins + On-off control valve***					
	- (T_{des} (°C),T_{cd} (°C)) = (70,10)	20.9	23.71	0.43	47.42	64.14
	- (T_{des} (°C),T_{cd} (°C)) = (80,10)	19.3	45.99	0.36	91.97	33.08
	- (T_{des} (°C),T_{cd} (°C)) = (90,10)	17.6	60.73	0.30	121.46	25.04
	- (T_{des} (°C),T_{cd} (°C)) = (80,5)	17.3	53.77	0.39	107.54	28.29
	- (T_{des} (°C),T_{cd} (°C)) = (80,15)	19.4	32.10	0.30	64.19	47.39
5.	***From Literatures (Range)*[6-8]**	5 - 20	-	0.14 – 0.76	35.0 – 521.3	2.0 - 6.7

4. CONCLUSION

The upright single-effect adsorption cooling system was experimented. The cooling rate of the adsorber influenced the system performance. Six cooling methods were tests, using either cooling water or internal thermosyphon heat pipes, or their combinations. Thermosyphon and CLOHP could enhance heat transfer as well as reduce cycle time. The adsorber was cooled down appropriately during cooling phase by integrating two methods that the shortest cooling time was achieved in the case of cooling water and CLOHP. The COP and SCP were mostly increased with desorption temperature but decreased with condensation temperature. VCP could be improved by increasing desorption temperature and decreasing cooling water temperature of the condensor. By incorporating simple procedures of the on-off self-control valve, the cooling power, COP, and SCP were not significantly reduced. In comparison with the other research works; the performance of our adsorption cooling system was noticeably equivalent.

5. ACKNOWLEDGMENTS

The authors gratefully acknowledge the support provided by the Thermal Technology Research Laboratory, Mae Moh Training Center, Electricity Generating Authority of Thailand (EGAT), Lampang, Thailand. We also acknowledge the Graduate School and Faculty of Engineering, Chiang Mai University (CMU), Thailand Research Fund (TRF), and the Commission on Higher Education, for their financial support.

6. REFERENCES

[1] Kim Choon Ng, Xiaolin Wang, Yee Sern Lim, Bidyut Baran Saha, Anutosh Chakarborty, Shigeru Koyama, Atsushi Akisawa, Takao Kashiwagi (2008) Experimental study on performance improvement of a four-bed adsorption chiller by using heat and mass recovery, *International Journal of Heat and Mass Transfer*, **49**, pp. 3343–3348.

[2] Katepradit Tanad (2003) *Thermosyphon Heat Exchanger World Energy Magazine*, 3.16.

[3] Piyanun Charoensawan (2003) Heat Transfer Characteristics of Closed-Loop Oscillating Heat Pipe. *Doctor of philosophy in mechanical engineering*. Graduate school. Chiang Mai University.

[4] Leong, K.C., Liu, Y. (2006) System performance of a combined heat and mass recovery adsorption cooling cycle: A parametric study, *International Journal of Heat and Mass Transfer*, **49**, pp. 2703–2711.

[5] Critoph R.E. (1988) Performance limitations of adsorption cycles for solar cooling, *Solar Energy*, **41**,(1), pp. 21-31.

[6] Wang L.W., Wang R.Z., Wu J. Y., Xu Y.X. and Wang S.G. (2006) Design, simulation and performance of a waste heat driven adsorption ice maker for fishing boat, *Energy*, **31**, pp. 244-259.

[7] Qu, T.F., Wang, R.Z. and Wang, W. (2001) Study on heat and mass recovery in adsorption refrigeration cycles, *Applied Thermal Engineering*, **21**, pp. 439-452.

[8] Wu, J.Y., Wang, R.Z. and Xu, Y.X. (2002) Experimental results on operating parameters influence for an adsorption refrigerator, *International Journal of Thermal Science.* **41**, pp. 137-145.

International Publications

1.4 Performance study on the consolidated adsorbent bed of activated carbon-methanol adsorption cooling system. International Conference on Green and Sustainable Innovation (ICGSI) 2009, 2-4 December 2009,Chiang Rai, Thailand.

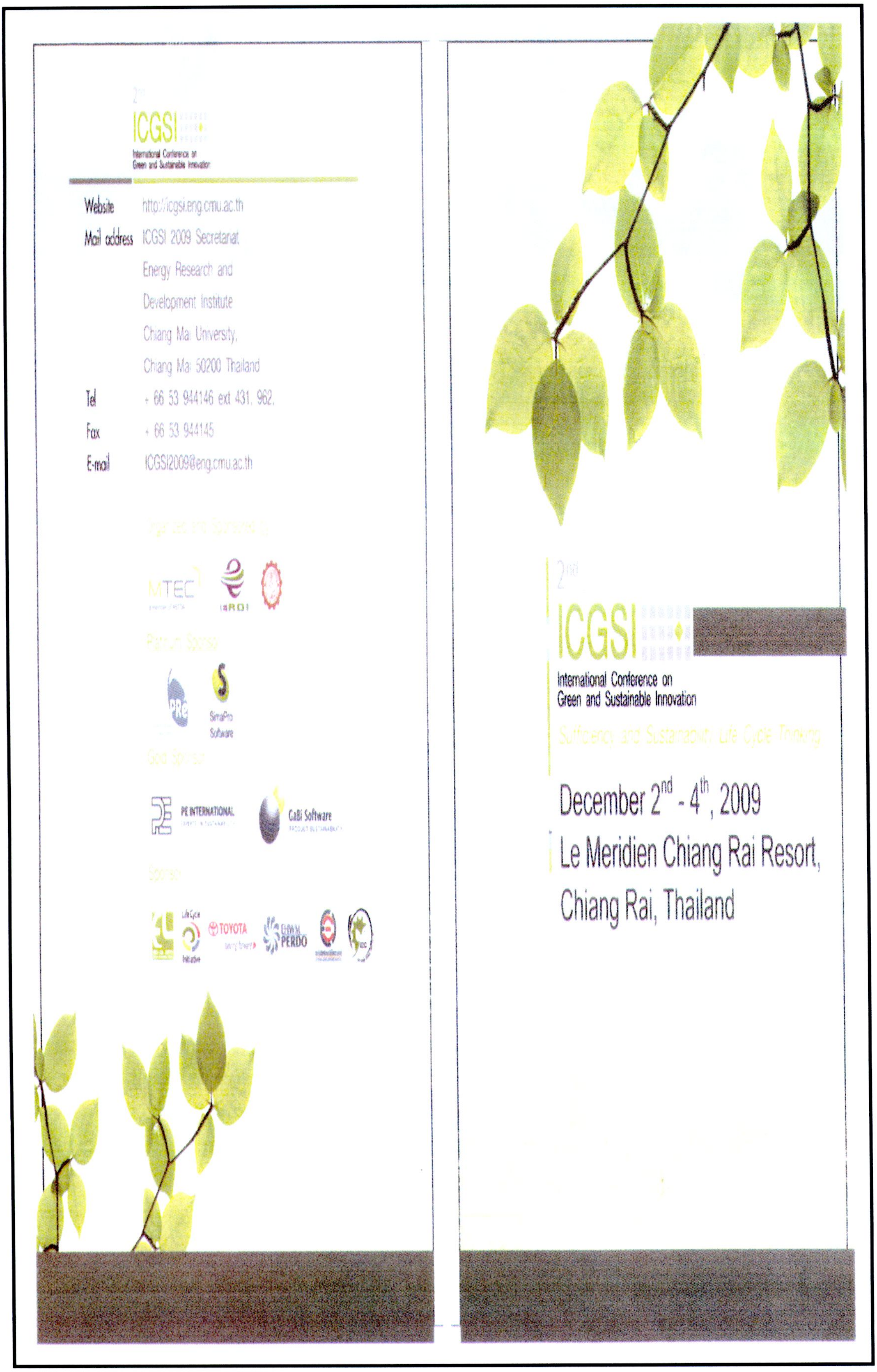

2nd
ICGSI
International Conference on
Green and Sustainable Innovation

Website http://icgsi.eng.cmu.ac.th
Mail address ICGSI 2009 Secretariat
Energy Research and
Development Institute
Chiang Mai University,
Chiang Mai 50200 Thailand
Tel + 66 53 944146 ext 431, 962,
Fax + 66 53 944145
E-mail ICGSI2009@eng.cmu.ac.th

Organized and Sponsored by

Platinum Sponsor

Gold Sponsor

Sponsor

2nd
ICGSI
International Conference on
Green and Sustainable Innovation

Sufficiency and Sustainability Life Cycle Thinking

December 2nd - 4th, 2009
Le Meridien Chiang Rai Resort,
Chiang Rai, Thailand

ICGSI

International Conference on Green and Sustainable Innovation 2009
December 2 – 4, 2009, Chiang Rai

Performance study on the consolidated adsorbent bed of activated carbon-methanol adsorption cooling system

Wipawadee Wongsuwan[1,*], Wirote Ritthong[1,3], Atipoang Nuntaphan[2], and Krit Toonkat[1]

[1]Energy Engineering Field of Study, Mechanical Engineering Department, Faculty of Engineering,
Chiang Mai University (CMU), 239 Huaykaew rd., Suthep, Muang, Chiangmai, Thailand, 50200.
Tel. +66 53 94 41 46 ext. 968, Fax. +66 53 94 41 45.

[2]Thermal Technology Research Laboratory, Mae Moh Training Center, Electricity Generating Authority of Thailand (EGAT),
Mae Moh, Lampang, Thailand, 52220.

[3]Rajamangala University of Technology Phra Nakhon, Department of MechanicalEngineering, Faculty of Engineering,
1381 Piboonsongkram Rd. Bangsue Bangkok 10800.

[*] Corresponding Author E-Mail Address: Wipawadee.w@gmail.com

Abstract

Adsorption cooling is an alternative system of air-conditioning and refrigeration. The system typically includes adsorber(s), an evaporator and a condenser. The adsorber containing adsorbent bed is the most important part, where cyclical adsorption and desorption takes place. The selected adsorbent/adsorbate (or working) pair was activated carbon (AC) and methanol. The adsorbent bed is usually required binder to enhance its consolidation into cylindrical or planer shape. We investigated appropriated binders to ease consolidation, forming stable bed, as well as to improve mass and heat transfer properties of adsorbent bed. The potential binders/additives to be used with AC type CGC-11A are; for example, methycellulose, polyvinylacetate (PVA), and graphite. The consolidated adsorbent bed was experimented for their adsorption capacities, thermal conductivity, and compressive strength. The best composition of consolidated bed was 2.5 % w/w of PVA to AC that gave high adsorption capacities about 35.9% ± 3.03% w/w under atmospheric condition and 27.36% v/w under vacuum condition, compressive strength about 0.66 MPa, and greatest durability within saturated methanol vapor. It has high thermal conductivity and effective thermal conductivity about 1.141 W.m^{-1}K^{-1} and 0.618 W.m^{-1}K^{-1}, respectively, and could be increased by 58% if the graphite additive is used. Therefore, the composite activated carbon bed for methanol adsorption should be consolidated by using PVA as binder and graphite as additive in order to enhance efficient adsorption cooling system.

Keywords: Adsorption cooling, Consolidated, Adsorbent bed, Activated carbon-Methanol

1. Introduction

Adsorption cooling system is environmental friendly which have zero ozone depletion due to the use of natural refrigerant, e.g. water, methanol and ethanol. The power consumption of this system is less than vapor compression, involved to noise, vibration and initial investment. Low grade of waste heat and solar energy is might be used as its heat source. Three major components of the system are adsorber, condenser and evaporator. The adsorber containing adsorbent bed is the most important part. The adsorbent bed is the combination of adsorptive materials (e.g. activated carbon, silica gel, zeolite, etc.) and non-adsorptive material (e.g. binder, additives, conductive material, support structure, fins, refrigerant channel, etc.). The adsorbent bed should be durable and enhance effective rate of heat and mass transfer that lead to better performance. Therefore, the adsorptive material within the bed must have high adsorption capacity and thermal conductivity. The granular AC was grinded to be AC powder having 100-200 mesh size that is normally loose and cannot maintain the desired shape without binder. Hence, various composite adsorbents combing activated carbon (AC) and eight chemicals including; functional carbon materials, binders and additives, have been consolidated and tested. One among popular working pair of adsorption cooling system is AC and methanol. The best combination and composition will be suggested for the AC/methanol adsorption cooling system.

AC has large adsorption capacity, range from 42.1% to 45.9% in case using binders. Although the maximum adsorption capacity measured for pure AC powder was 42.8% - 47.2% [1]. Low desorption heat source is the advantage of this working pairs, so that solar energy and waste recovery heat sources are possibly supply to the system.

The potential binders/additives are selected based on information from literatures as well as results from our previous research work [2]. The heat transfer property of the bed is also important. Pure AC has thermal conductivity within the range of 0.15 - 0.50 $W.m^{-1}K^{-1}$ [3]. For the AC-methanol pair, PTFE (polytetrafluoroethylene) was added to AC providing 0.13-0.2 $W.m^{-1}K^{-1}$ effective thermal conductivity [1]. The polyvinyl alcohol mixed with polyethylene glycol in AC with graphite additive for methane adsorption resulted in 2-8 $W.m^{-1}K^{-1}$ of thermal conductivity [4]. Furthermore, various types of chemical binder are used to maintain the stability of adsorbent bed, e.g. cement in calcium chloride using AC as additive to reduce an agglomeration of calcium chloride bed [5], calcium chloride with cement binder using AC additive having weight ratio of calcium chloride/AC/cement about 16:4:1 providing system COP up to 0.39 [6], bentonite bonded to zeolite particles having excellent heat transfer in shell and tube heat exchanger [7], carboxymethyl cellulose composed to AC for phenol adsorption [8]. Bulky graphite binder enhanced uniformity of reactive salt distribution in chemical adsorption between sodiumsulphide salt and water vapor [9].

The AC powder and binders are mixed and consolidated to form composite material. The composite adsorbent beds are expected to have high adsorption capacity of methanol vapor during either adsorption or desorption phase, and high thermal conductivity for heat transfer between bed and adsorber wall. Our research activity is focused on preparing the stable adsorbent bed that offer high adsorption capacity. In this work, composite adsorbent beds are consolidated from AC and eight types of binder/additive with various compositions. Therefore, results on their adsorption capacities, bed stability and thermal conductivity are presented and discussed.

2. Experimental

2.1 Composite AC adsorbent bed

Activated carbon (AC) from coconut shell type CGC-11A, having 1,000 m^2/g surface area and 100-200 mesh size, was consolidated to form the adsorbent bed by using binder. Eight types of binder and additive are mixed with AC; i.e. bentonite, cement, cement with graphite, plaster of paris, calciumcarbonate, calciumhydroxide, methylcellulose, and polyvinylacetate (PVA). Binder facilitates formation and stability of adsorbent bed. Additive assists mass and/or heat transfer properties of bed. Methylcellulose can be classified into either additive or binder. However, graphite and methylcellulose are categorized as additive, so that the rest are categorized as binder. To simplify, this paper refers to all 'filler chemicals' as binder.

Consolidation of AC bed is produced by compressing the composite powder prepared by mixture of AC and binders. The advantage of consolidated adsorbent bed is the high thermal conductivity in the direction perpendicular to the compression [1]. The manufacturing procedure of the consolidated composite AC is as following [10]:

1) Binder is added to AC powder.
2) Mixture is filled by water droplets so that the slurry is created.
3) The well mixed mixture is molded by compression in cylindrical mold to form cylinder having 15 mm diameter and 18 mm height.
4) The consolidated composite adsorbent is obtained after drying at 60 °C for 24 hours to remove moisture content.

Fig. 1 illustrates the consolidation procedure of the composite AC bed. In the first experiment, various combinations were made of AC/binder mixture in mass ratio varied by 5, 10, 15 and 20% of binders to AC. All samples contained similar AC mass approximately 2 g. The consolidated composite AC beds were observed for their uniformity, shape deformation, powder loosing, and durability, without any force applied to the bed. Most of bed samples generally compromised its function as adsorbent bed, in terms of uniformity and stability.

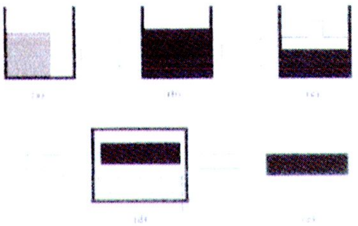

Fig. 1 Manufacturing procedure of consolidated composite adsorbent (a) AC mixed with binder; (b) Slurry of mixture and water; (c) Compressing; (d) Drying at 60°C for 24 hours; (e) Consolidated composite adsorbent bed.

2.2 *Adsorption capacity of composite adsorbent bed*

The adsorption capacity of the composite materials in atmospheric condition is defined as the maximum amount of adsorbed methanol to dry AC weight. The experiment on adsorption process was done in the closed-glass chamber. At the beginning, the composite AC bed was measured its weight, putted into opened-plastic container. Next, the bed within plastic container was placed on the cotton inside glass chamber, and then glass chamber was closed. Environment of saturated methanol vapor was generated by vaporization of methanol from methanol-soaked cotton. The chamber was placed in an atmospheric environment, temperature (27°C – 28 °C) and relative humidity (85% - 95%), for 72 hours until the equilibrium condition has been reached. The adsorption process between AC and methanol occurs by filling and condensation of adsorbate inside adsorbent pores, mainly in micropores (0.15 – 0.50 $cm^3 g^{-1}$ specific volume) [1]. However, middle pores and large pores only transport the methanol molecules to micropores. The difference of mass before and after adsorption was the adsorbed mass of methanol vapor

Consequently, under vacuum condition (21-35 kPa), the adsorption capacity was experimented in the adsorption test bench, designed in similar configuration to Ref. [10]. The adsorption unit was consisted of two chambers, an adsorber and an evaporator/condenser, which made of stainless steel. The vertical 12.5-mm diameter tube was for methanol vapor passage (Fig. 2). The 200-ml adsorber in the upper part contains the adsorbent bed, and places inside the water jacket. A water coolant is circulated in the jacket to collect heat during the adsorption process. The evaporator/condenser provides evaporation and condensation functions as well as storage of methanol. The residual volume of methanol inside the evaporator/condenser was calculated from its measured level. It was done by 'hall effect sensor' detecting the magnetic field. The piece of magnetic was float up and down in corresponding with the change of methanol level.

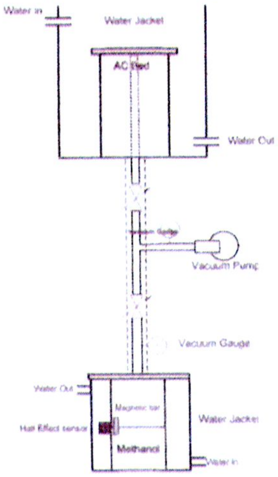

Fig. 2 Test bench of adsorption capacity

2.3 Thermal conductivity

The thermal conductivity measurement were performed under transient condition, by hot-wire method [11]. The adsorbent bed temperature was increased due to the input electrical current. The adsorbent bed and the container must have particular geometries respected to ISO 8894-2: Determination of thermal conductivity-Hot wire method (paralled), with geometry 200 × 100 × 50 mm. The measuring probe consists of two nickel chromium-nickel aluminum thermocouples and a very thin nickel chromium straight heating wire with 0.3-mm diameter [12]. During the test, the thermocouple and heating wire were fixed in the bed as shown in Fig. 3 and a complete measurement circuit is shown in Fig. 4.

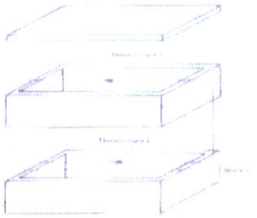

Fig. 3 Adsorbent bed container and thermocouple position within the bed.

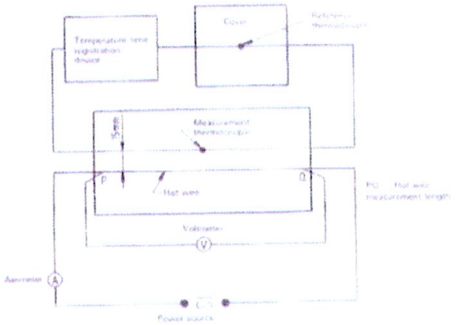

Fig. 4 Electrical circuit of thermal conductivity measurement.

The metal wire was supplied and heated by constant electrical current. Temperature, electrical current and voltage at different time were measured and recorded. The thermal conductivity can be calculate by [12]

$$\lambda = \frac{IV}{4\pi l} \times \frac{-E_i\left(\frac{-r^2}{4at}\right)}{\Delta\theta(t)} \qquad (1)$$

where; I is the electrical current, V is the electrical voltage, l is the length of the hot wire, $\Delta\theta(t)$ is the temperature different between point 1 and 2 (in Fig. 3) at time t, r is the distant between the hot wire and the measuring thermocouple, α is the thermal diffusivity. $-E_i\left(\frac{-r^2}{4\alpha t}\right)$ is the exponential integral function of $\int_{\frac{r^2}{4\alpha t}}^{\infty}\frac{e^{-\eta}}{\eta}d\eta$, which can be read from the Ref.[11] in corresponding with $\frac{\Delta\theta(2t)}{\Delta\theta(t)}$.

The effective thermal conductivity of porous adsorbent can be calculated by [12]

$$\lambda_{eff} = (1-)\lambda_s + \varepsilon\lambda_g \qquad (2)$$

where ε is the porosity of the adsorbent, λ_s and λ_g are the thermal conductivities of the solid adsorbent and vapor, respectively.

2.4 Durability and compressive strength

The composite adsorbent beds with various combinations and compositions were tested for their durability and stability (or resistance to shape deformation). The cylindrical adsorbent beds having 15-mm diameter and 20-mm height were encapsulated within methanol vapor for 90 days.

In addition, the adsorbent beds were tested for the compressive strength by Universal testing machine which follows by ASTM; Standard test method for compressive strength of carbon and graphite [13]. The compressive strength illustrated the bed endurance under the applied force over unit area. According to ASTM, the bed in cylindrical shape has 9-mm diameter and 19-mm height, with the ratio of height to diameter between 1.9 and 2.1. The results were obtained as the maximum compressive force (in MPa) applied to the adsorbent bed until their collapses.

3. Results and Discussions

3.1 Adsorption capacity in atmospheric condition

The adsorption capacities in term of adsorbed methanol to AC (%w/w) for the bed using various types of binder are shown in table 1. The higher mass ratio of binder almost resulted in lower adsorption capacity, due to increasing possibility of pores occlusion [1]. Therefore, we conclude that the mass ratio approximately 5% to 10% is sufficient to maintain the adsorbent bed in cylindrical shape without collapse.

Next, the experiment was repeated with appropriated mass ratio of binder to AC, just sufficient to maintain shape of composite bed stability as shown in Fig. 5.

Most of the combinations gave lower adsorption capacities than the pure AC. The reduction of adsorption capacity due to composite with binder was between 2.50% - 6.73%. In contrary, the case of methylcellulose 5% could achieve 2.06% higher adsorption capacity. This combination also gave highest adsorption capacity, approximately 40.55% ± 0.88% by mass of methanol to adsorbent material. As mentioned above, methylcellulose could assist bed with both functions of binder and additive simultaneously.

Table 1. Adsorption capacities with eight compositions in 5%-20% ratio of binder to AC

Binder type	Adsorption capacity (% w/w)			
	5	10	15	20
Methyl Cellulose	34.8	35.6	44.6	44.0
Polyvinyl acetate	39.5	36.5	30.1	37.5
Cement+ Graphite 5%	38.7	34.8	31.4	25.4
Cement	45.4	39.4	36.1	34.1
Calciamhydroxide	34.6	37.0	27.0	29.5
Plaster of paris	34.1	32.9	31.2	30.0
Calciamcarbonate	30.3	37.2	35.2	34.4
Bentonite	40.5	36.6	39.5	34.1
Average	37.3	36.2	34.4	33.6
Standard deviation	11.6	8.9	8.4	7.0

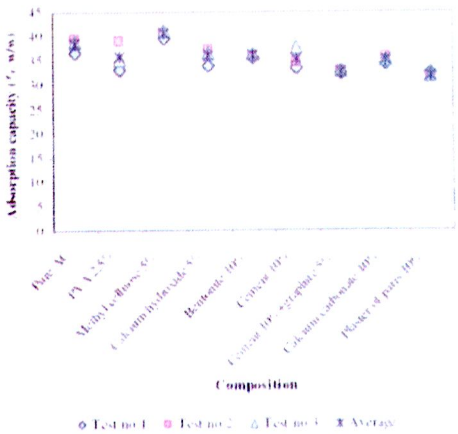

Fig. 5 Adsorption capacities with appropriated binder to AC.

3.2 *Durability and strength of adsorbent bed*

Adsorbent beds having eight combinations of binder to AC were placed in the chamber and surrounded by saturated methanol vapor for 90 days, to illustrate their stable physical characteristic. The result show that the bed having bentonite and PVA as binder had no evidence of erosion. The rest had lost their mass around 5%-30% of AC. Unfortunately, the methylcellulose binder was obviously separated from AC. The bed having calciumcarbonate as binder was collapsed. Hence, methylcellulose and calciumcarbonate could not be used to strengthen the composited adsorbent bed.

The test of compressive strength based on ASTM standard [13] of the beds was repeated for three times to ensure the strength of each combination. In Table 2, methylcellulose as binder gave the average highest strength about 2.82 MPa, followed by PVA and Bentonite, respectively. In comparison, PVA and Bentonite efficiently helped to consolidate the bed without losing any AC powder.

Table 2. Compressive strength of the composite adsorbent bed in several binders.

Binder		**Average Compressive Strength (MPa)**
Methylcellulose	5% w/w	2.82
PVA 2.5% w/w with graphite	5 % w/w	1.17
PVA	2.5 % w/w	0.66
Bentonite	10 % w/w	0.24
Plaster of paris	10 % w/w	0.10
Calciumhydroxide	5 % w/w	0.03
Calciumcabonate	10 % w/w	0.03
Cement	10 % w/w	0.01
Cement 10% w/w with graphite	5 % w/w	0.01

3.3 *Adsorption capacity in vacuum condition*

The selected composited was tested for their cyclical adsorption capacities under 21 kPa adsorption and 24-35 kPa desorption pressures. In adsorption period, the temperature of the adsorber and evaporator were set to 23-25 ^{o}C and 28-30 ^{o}C. In desorption period, the temperature of the adsorber and condenser were set to 97-105 ^{o}C and 0-3 ^{o}C, respectively. Each specimen was repeating tested for three adsorption cycles.

Fig. 6 showed that the highest adsorption capacity was found in the first cycle. It drastically decreased in the following second and third cycles. The adsorbed and desorbed amount was largely difference as well. The reason was that the beds are not yet break-through at that state. The highest adsorption capacity about 27.26% v/w in the first cycle was found from the bed having PVA binder.

To ensure the breaking-through state, the bed having PVA was repeated its adsorption test for 20 cycles. The cycle no. 9 to 20 gave similar adsorbed/desorbed amount of having consistency adsorption capacity. We could summarize that the break-through of the bed started from cycle number 9. Also, we suggested that the adsorbent bed must be readily pretreated by at least 9 adsorption cycles prior to the use in any adsorption cooling system.

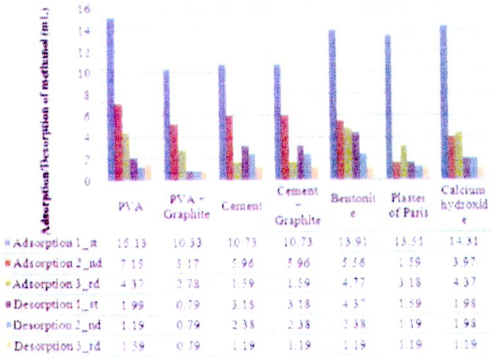

Fig. 6. Adsorption capacities of the adsorbent with seven compositions under vacuum condition.

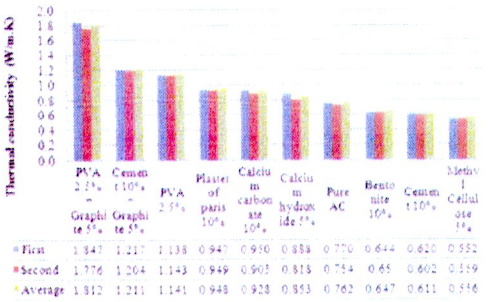

Fig. 7 Thermal conductivity of the composite adsorbent bed having various binder and additive.

3.4 Effective thermal conductivity.

The thermal conductivity of the several composite bed combinations based on ISO8894-2 [11] gave results as shown in Fig. 7. The bed having PVA binder gave the thermal conductivity about 1.141 $Wm^{-1}K^{-1}$ and effective thermal conductivity of 0.618 $Wm^{-1}K^{-1}$.

Especially, the bed having 'graphite' as additive and having PVA and cement as binder, their thermal conductivities (1.812 $Wm^{-1}K^{-1}$ and 1.211 $Wm^{-1}K^{-1}$, respectively) were increased by 58% and 98% from the case without graphite. Therefore, 'graphite' could improve bed thermal conductivity significantly. However, the addition percentage of the graphite additive should not lessen the adsorption capacities.

4. Conclusion

The composite adsorbent bed of AC/methanol pair was formed by using eight binder and additive, with different combinations and composition, to improve their heat and mass transfer characteristics. It has shown possibility to prepare cylindrical AC bed with uniformity and stability. The adsorption capacity is slightly affected by the presence of binder/additive. The experimental adsorption quantities obtained were comparable to maximum adsorption mass of AC/methanol in literatures. Among potential binders/additives in use, the best composition was 2.5 % w/w of PVA to AC that gave high adsorption capacities with 35.9% ± 3.03% w/w in atmospheric condition and gave 27.36% v/w in vacuum condition, compressive strength about 0.66 MPa, and the best durability in saturated methanol vapor. It has higher thermal conductivity and effective thermal conductivity about 1.141 $W.m^{-1}K^{-1}$ and 0.618 $W.m^{-1}K^{-1}$, respectively as compared to the other. The graphite additive could also increase thermal conductivity up to 58%. In brief, the composite activated carbon bed for methanol adsorption should be consolidated by using PVA as binder and graphite as additive to enhance efficient adsorption cooling system.

5. Acknowledgement

The authors would like to acknowledge research grants from the Graduate School and the Mechanical Engineering Department, Chiang Mai University (CMU). We also thank the Commission on Higher Education, and Thailand Research Fund, for their financial support.

6. References

[1] Cacciola, G., Restuccia, G., and Mercadante, L., (1995). Composites of activated carbon for refrigeration adsorption machines. *Carbon*, Vol. 33, No. 9, pp. 1205-1210.

[2] Toonkat, K., Wongsuwan, W., Kiatsiriroat, T., (2009). The effect of chemical additives on the performance of activated carbon adsorbent bed, *PACCON 2009: Proceedings on Pure and Applied Chemistry International Conference 2009*, January 14-16, 2009, Naresuan University, Phitsanulok, Thailand, pp. 214-217.

[3] Py X., Menard D. and Mazet N. (2005). Activated carbon monolith of high thermal conductivity for adsorption processes improvement. Part A: Adsorption step. *Chemical Engineering and Processing*, vol. 44, pp.1029 – 1038.

[4] Biloe, S., Boetz, V., and Mauran, S., (2001). Characterization of adsorbent composite blocks for methane storage. *Carbon*, Vol.39, pp. 1653 – 1662.

[5] Wang L.W., Wang R.Z., Wu J.Y. and Wang K., (2004). Compound adsorption ice maker on fishing boats. *Journal of Refrigeration*, Vol. 27, pp. 401-408.

[6] Lu Z.S., Wang R.Z., Wang L.W and Chen C.J., (2006). Performance analysis of refrigerator using activated carbon in a compound adsorbent. *Carbon*, Vol. 44, pp. 147-752.

[7] Restuccia G., Freni A., Russo F. and Vasta S., (2005). Experimental investigation of a Solid adsorption chiller based on a heat exchanger coated with hydrophobic zeolite. *Applied Thermal Engineering*, Vol. 25, pp.1419-1428.

[8] Nestor Tancredi, Natalia Medero, Fabiana Moller, Javier Piriz, Carina Plada and Tomas Cordero., (2004). Phenol adsorption onto powdered and granular activated carbon prepared from Eucalyptus wood, *Journal of Colloid and Interface Science*, Vol. 279, pp. 357-363.

[9] Kantima Iammak, Wipawadee Wongsuwan, and Tanongkiat Kiatsiriroat, (2004). Investigation of modular chemical energy storage performance. *The Joint International Conference on Sustainable Energy and Environment (SEE)*, 1-3 December 2004,Hua Hin, Thailand.

[10] Dellero T., Sarmeo D., Touzain Ph., (1999). A chemical heat pump using carbon fibers as additive. Part I: enhancement of thermal conduction. *Applied thermal engineering*, Vol. 1, pp. 991-1000.

[11] Refractory material (1990). Determination of thermal conductivity-Hot wire method (paralled), s0022839-ISO8894-2, TISI Library Thailand.

[12] Wang K, Wu J.Y., Wang R.Z., Wang L.W. (2006). Effective Thermal conductivity of expanded graphite-$CaCl_2$ composite adsorbent for chemical adsorption chillers. *Energy conversion and management*, Vol.47, pp. 1902-1912.

[13] American Society for Testing and Materials (ASTM)(1993). Standard test method for compressive strength of carbon and graphite. Vol. 15-01, C 695-91.

CIRRICULUM VITAE

Name	Mr. Wirote Ritthong
Date of birth	May 8, 1973
Education	M. Eng. degree in Mechanical Engineering from Chiang Mai University (CMU) in 2000 B. Eng. degree in Mechanical Engineering from Rajmangala University of Technology Thanyaburi (RMUTT) in 1996
Specialist	Refrigeration and Air Conditioning System, Design Thermal System and Alternative Energy.
Contact address	Department of Mechanical Engineering, Rajchamangala University of Technology Phra Nakhon (RMUTP) 1381 Piboonsongkam Road, Bangsui, Bangkok 10800 Tel: (66)2913-2424 Ext. 168 Mobile: (66)8912-98233 Email: wrritthong@gmail.com

Publication

(1) Ritthong W., Kiatsiriroat T., Wongsuwan W. and Nuntaphan A. **"Performance analysis of a modular adsorption cooling system with sonic vibration in the adsorber"** Paper accepted for publication in Journal of Experiment Heat Transfer, 10 May 2011, (Article inpress).

(2) Wongsuwan W., Ritthong W., Nuntaphan A. and Kiatsiriroat T. **"Performance analysis of a modular adsorption cooling system having sonic vibration at evaporator"** Paper accepted for publication in ASCE's Journal of Energy Engineering, vol. 137, No. 2, June 1, 2011.

(3) Wongsuwan W., Ritthong W., Nuntaphan A. and Toonkat K. **"Performance study on the consolidated adsorbent bed of activated carbon-methanol adsorption cooling system"** International Conference on Green and Sustainable Innovation (ICGSI) 2009, 2-4 December 2009,Chiang Rai, Thailand.

(4) Ritthong W., Jansatidpaiboon P., Aim-eiam T., Wongsuwan W., Nuntaphan A. and Kiatsiriroat T. **"Performance Analysis of Thermosyphon Assisted Adsorption Cooling System"** World Renewable Energy Congress 2009-ASIA. The 3rd International Conference on "Sustainable Energy and Environment (SEE 2009)", 18-23 May 2009, Bangkok, Thailand.